Original Article

Assessing non-linearity in European temperature-sensitive tree-ring data

Fredrik Charpentier Ljungqvist[a,b,c,*], Peter Thejll[d], Jesper Björklund[e], Björn E. Gunnarson[f,b], Alma Piermattei[g], Miloš Rydval[h], Kristina Seftigen[i,j,e], Bård Støve[k], Ulf Büntgen[g,e,l,m]

[a] *Department of History, Stockholm University, 106 91 Stockholm, Sweden*
[b] *Bolin Centre for Climate Research, Stockholm University, 106 91 Stockholm, Sweden*
[c] *Swedish Collegium for Advanced Study, Linneanum, Thunbergsvägen 2, 752 38 Uppsala, Sweden*
[d] *Danish Meteorological Institute, Lyngbyvej 100, 2100 Copenhagen Ø, Denmark*
[e] *Dendro Sciences Group, Swiss Federal Research Institute WSL, 8903 Birmensdorf, Switzerland*
[f] *Department of Physical Geography, Stockholm University, 106 91 Stockholm, Sweden*
[g] *Department of Geography, University of Cambridge, Cambridge CB2 1QB, United Kingdom*
[h] *Forestry and Wood Sciences, Department of Forest Ecology, Czech University of Life Sciences Prague, 16500 Prague, Czech Republic*
[i] *Regional Climate Group, Department of Earth Sciences, University of Gothenburg, 405 30 Gothenburg, Sweden*
[j] *Georges Lemaître Centre for Earth and Climate Research, Université catholique de Louvain, 1348 Louvain-la-Neuve, Belgium*
[k] *Department of Mathematics, University of Bergen, Johannes Brunsgate 12, 5008 Bergen, Norway*
[l] *CzechGlobe Global Change Research Institute CAS, 603 00 Brno, Czech Republic*
[m] *Department of Geography, Faculty of Science, Masaryk University, 613 00 Brno, Czech Republic*

ARTICLE INFO

ABSTRACT

We test the application of parametric, non-parametric, and semi-parametric calibration models for reconstructing summer (June–August) temperature from a set of tree-ring width and density data on the same dendro samples from 40 sites across Europe. By comparing the performance of the three calibration models on pairs" of tree-ring width (TRW) and maximum density (MXD) or maximum blue intensity (MXBI), we test whether a non-linear temperature response is more prevalent in TRW or MXD (MXBI) data, and whether it is associated with the temperature sensitivity and/or autocorrelation structure of the dendro parameters. We note that MXD (MXBI) data have a significantly stronger temperature response than TRW data as well as a lower autocorrelation that is more similar to that of the instrumental temperature data, whereas TRW exhibits a redder" variability continuum. This study shows that the use of non-parametric calibration models is more suitable for TRW data, while parametric calibration is sufficient for both MXD and MXBI data – that is, we show that TRW is by far the more non-linear proxy.

1. Introduction

Tree-ring data play a central role for reconstructing temperature and hydroclimate variability over the past one to two millennia (Cook et al., 2004, 2010, 2015; Esper et al., 2016, 2018; Ljungqvist et al., 2016, 2019b,a; Wilson et al., 2016; Anchukaitis et al., 2017). This palaeoclimate archive has a strong advantage due to its annual resolution and absolute dating accuracy (Schweingruber, 1988; Cook and Kairiukstis, 1990; Büntgen et al., 2018) in combination with relatively good knowledge of the biological processes governing tree growth (Fritts, 1976; Speer, 2010; Anchukaitis, 2017). The most frequently and successfully used tree-ring parameters for the study of past temperature variation are tree-ring width (TRW) and maximum latewood density (MXD) (e.g. Esper et al. (2016, 2018)). TRW contains considerable variability obscuring climatic

information, such as age and size related trends (Cook and Kairiukstis, 1990; Weiner and Thomas, 2001), biological memory effects (Fritts, 1976; Esper et al., 2015), and external disturbances (Rydval et al., 2018) whereas MXD appears to be less affected by non-climatic interference (Briffa et al., 2004) – resulting in a generally stronger temperature signal in MXD data than in TRW data (Kirdyanov et al., 2007; Büntgen et al., 2011; Konter et al., 2016). Recently, techniques using reflected light from the surface of wood (blue intensity) (see Appendix A) as a surrogate for the X-ray derived MXD has shown promising results (Wilson et al., 2017a), both in terms of replicating variability of the MXD parameter by using the corresponding maximum blue intensity (MXBI) parameter (Björklund et al., 2014), and in terms of its ability to reconstruct temperature (Kaczka et al., 2018).

Almost all tree-ring records are influenced, to a greater or lesser

---

extent, by *both* growing season temperature and hydroclimatic conditions (Babst et al., 2013; St George and Ault, 2014; St George, 2014; Klesse et al., 2018). However, the response to either temperature or hydroclimate may be strongly dominating for tree-ring data from certain locations allowing the reconstruction of one of the parameters. This typically occurs at the extreme limit of a tree species' distribution where climate may strongly dominate tree growth at certain locations, allowing the reconstruction of either temperature or hydroclimate from the tree-ring data (Hellmann et al., 2016). However, even at such locations, the strength of the response is typically unstable over time (Büntgen et al., 2013; Galván et al., 2014; Schultz et al., 2015; Seim et al., 2016; Babst et al., 2019).

For various reasons, including those mentioned above, the relationship between tree growth and climate can often be of a non-linear nature (for definitions of non-linearity, see Section 3). The most well-known example of such non-linear tree-growth behaviour is the "divergence problem" (Wilson et al., 2007; D'Arrigo et al., 2008): the apparent weakening – or even negative – response of temperature-sensitive tree-ring chronologies to temperature, and/or trend departure, since around the 1970s (Jacoby and D'Arrigo, 1995). A temperature disassociation with tree growth has been identified for both TRW and MXD, mainly affecting the low-frequency signal and trend (Briffa et al., 1998), although a reduced high-frequency sensitivity has also been reported (D'Arrigo et al., 2008).

Especially in regions where climate is not the main limiting factor for tree growth, multiple factors can influence tree growth and introduce non-linearities, ranging from forest management (He et al., 2016), stand competition (Cook, 1985), and insect outbreaks (Esper et al., 2006; Büntgen et al., 2009) and so forth. The climate signal in tree-ring records can also be affected by natural and anthropogenic changes in the forest cover even at apparently pristine sites (Gunnarson et al., 2012). An additional potential, and poorly constrained, non-linear effect on the tree growth–climate relationship in modern times is the CO_2 fertilization effect (Graybill and Idso, 1993; Keenan et al., 2013; Zhu et al., 2016) that may recently artificially have enhanced growth for some tree species and in certain locations (Körner et al., 2007; Frank et al., 2015; Scharnweber et al., 2019).

Another factor to consider, of relevance in any assessment of non-linear climate–tree growth relationships, is that tree-ring data contain a different autocorrelation structure than their instrumental target data – something that can constitute unexplained variance. This was already, for TRW, highlighted by Schulman (1956) and Matalas (1962). It appears as though TRW data exhibit a larger biological carry-over effect (Frank et al., 2007) due to the utilisation of carbohydrates from previous year(s) (Vaganov et al., 2006) than MXD data (Schweingruber et al., 1978; Björklund et al., 2017), leading to TRW data containing a considerably "redder" variability continuum than instrumental observations and MXD data (Bunde et al., 2013; Franke et al., 2013; Büntgen et al., 2015; Esper et al., 2015; Zhang et al., 2015).

While the non-linear temperature response in tree-ring data has been addressed in numerous publications – and differences in the temperature correlation strength and autocorrelation structure between TRW and MXD have been discussed as well – these issues have not hitherto been treated together in a systematic way. In particular, the issue of whether non-linear temperature responses in TRW data are more prevalent than in MXD data has never been thoroughly tested. Støve et al. (2012) tested the use of a mixture of parametric and non-parametric calibration methods upon a set of annually resolved temperature-sensitive proxy data, of which 19 were tree-ring records out of 30 proxies. Moreover, Støve et al. (2012) explored the potential benefits of applying a semi-parametric calibration method on proxy data exhibiting various degrees of non-linear response to temperature. The particular non-linear relationship between temperature and a tree-ring record represents a deterministic relationship (i.e. an exact relationship between the two variables). In reality, the relationship between temperature and tree-ring data (or other proxies) is non-deterministic for a

number of reasons, several of which are not handled by the testing procedure or the conceptual framework of the deterministic non-linear relationship. The method by Støve et al. (2012) for detecting non-linearity works best when using "pairs" of data, making it possible to compare which record of the two behaves *more* non-linear than the other. In this case, the need for "pairs" of data requires the use of a compromise target season – e.g. June–August – for the TRW, MXD, and MXBI data despite a shorter seasonal response for the former data type and a longer one for the latter data types (see further Section 5.2).

Here, we expand on the work of Støve et al. (2012) and test the use of parametric, non-parametric, and semi-parametric calibration methods upon a set of TRW, MXD, and MXBI data from identical tree-ring samples from 40 sites across Europe. We further explore whether the incidence of detected non-linearity is associated with the temperature correlation strength and/or the autocorrelation of the data. We explicitly pose the following testable questions: (1) Are MXD (MXBI) data more linear in their response to temperature than TRW data? (2) Is the potential linearity/non-linearity of TRW, MXD, and MXBI data, respectively, related to the strength of the temperature signal and/or autocorrelation structure? (3) Can the response of MXBI and MXD be distinguished from each other in their relationship with TRW?

2. Data

2.1. Tree-ring temperature-sensitive data

We have compiled published tree-ring temperature-sensitive data for Europe from locations where such chronologies exist both for TRW *and* MXD *or* MXBI (or for all three) covering the period 1860–2000 (Table 1; Fig. 1). The aim has been to compile records to provide a representative coverage, with northern Scandinavia serving as the principal test bed, but not to include all existing "pairs" of TRW and MXD (MXBI) data. A large number of additional TRW and MXD records are available, in particular from the Alps (Frank and Esper, 2005), but these records unfortunately end prior to the year 2000. Our data compilation consists of 32 "pairs" of TRW and MXD data and of 13 "pairs" of TRW and MXBI data. For practical purposes, we have grouped the tree-ring records into four regions: Scandinavia, Scotland, Continental Europe (the Alps and Tatra Mountains), and the Pyrenees (Table 1; Fig. 2).

A cubic smoothing spline (Cook and Peters, 1981, 1997) with a 50% frequency-response cut-off equal to 300 years were applied to remove non-climatic age trends from the raw TRW, MXD, and MXBI measurement series. This procedure limits the amount of low-frequency climate information preserved (Cook et al., 1995) compared to Regional Curve Standardisation (Esper et al., 2003) and related "signal free" (Melvin and Briffa, 2008) detrending techniques. However, this is of little importance here as we only consider temperature variability over the 141-year period 1860–2000 (see further Section 5.1). No special adjustment (Frank et al., 2007) was made for temporal variance changes between the individual series in each chronology. The indexed series were derived with division for TRW data and subtraction for MXD and MXBI data (Bräker, 1981; Schweingruber et al., 1988). Finally, the chronologies were produced by using the bi-weight robust mean (Hoaglin et al., 1983) in the program ARSTAN (Cook and Krusic, 2005). Only for TRW data from Scotland, some individual series were standardised using a 100-year spline to avoid a negative trend or a false positive trend at the end of the series. A number of individual measurement series in the Scotland MXBI data were deleted due to several zero values (e.g. 4 time series for Glen Derry North [GDN], 14 in Glen Falloch [GLF], 3 in Inverey [INV], 2 in Quoich [QUO], and 7 in Rhiddoroch [RHD]). Based on a disturbance assessment by Rydval et al. (2016) for all the Scottish data, only those site chronologies for which the disturbance effect was found to be minimal were included in this study. The sample depth and the Expressed Population Signal (EPS; Wigley et al. (1984)) values were calculated using the program ARSTAN (Cook and Krusic, 2005). The EPS was measured in standardised time-series

Table 1
List of tree-ring records included in this study (listed after latitude from north to south). The abbreviation code for tree species follows the standard used in the International Tree-Ring Data Bank (ITRDB) as listed in Grissino-Mayer (1993) as follows: LADE = European larch (*Larix decidua* Mill.), PCAB = Norway spruce (*Picea abies* (L.) H. Karst.), PICE = Swiss stone pine (*Pinus cembra* L.), PISY = Scots pine (*Pinus sylvestris* L.), and PIUN = Mountain pine (*Pinus uncinata* Ramond ex DC.). Other abbreviations: Long. = longitude; Lat. = Latitude; Elev. = elevation above sea level; TRW = tree-ring width; MXD = maximum latewood density; MXBI = maximum blue intensity. A "X" mark indicates the presence of data and a dash (–) indicates the absence of data.

Record	Long.	Lat.	Elev. (m)	Species	TRW	MXD	MXBI	Key reference
Scandinavia								
Northern Finland	28.20	68.90	200	PISY	X	X	X	Björklund et al. (2019)
Forfjorddalen	15.73	68.79	40–160	PISY	X	X	–	McCarroll et al. (2013)
Kiruna (KID)	20.17	68.50	430	PISY	X	X	–	Büntgen et al. (2011)
Kiruna (KIW)	20.17	68.50	430	PISY	X	X	–	Büntgen et al. (2011)
Ketomella (PTD)	24.08	68.37	300	PISY	X	X	–	Büntgen et al. (2011)
Ketomella (PTK)	24.08	68.37	300	PISY	X	X	–	Büntgen et al. (2011)
Ketomella (PTW)	24.08	68.37	300	PISY	X	X	–	Büntgen et al. (2011)
Laanila[a]	27.35	68.49	220–310	PISY	X	X	–	McCarroll et al. (2013)
Torneträsk (TOD)	19.80	68.33	390	PISY	X	X	–	Büntgen et al. (2011)
Torneträsk (TOW)	19.80	68.33	390	PISY	X	X	–	Büntgen et al. (2011)
Kesänkijärvi (KES)	24.50	67.93	450	PISY	X	X	–	Büntgen et al. (2011)
Luosu (PIS)	24.25	67.83	300	PISY	X	X	–	Büntgen et al. (2011)
Luosu (PIT)	24.25	67.83	300	PISY	X	X	–	Büntgen et al. (2011)
Muddus	20.30	66.90	450–510	PISY	X	X	–	Björklund et al. (2019)
Tjeggelvas	17.16	66.60	460–580	PISY	X	X	–	Björklund et al. (2014), Linderholm et al. (2015)
Arjeplog	18.20	66.30	550–700	PISY	X	X	X	Björklund et al. (2014), Linderholm et al. (2015)
Ammarnäs	16.10	65.90	400–600	PISY	X	X	–	Björklund et al. (2014), Linderholm et al. (2015)
Kittelfjäll	15.50	65.20	530–600	PISY	X	X	–	Björklund et al. (2014), Linderholm et al. (2015)
Jämtland	13.50	63.20	650–680	PISY	X	X	X	Björklund et al. (2014), Linderholm and Gunnarson (2019)
Rogen	12.40	62.37	700–900	PISY	X	–	X	Fuentes et al. (2018)
Scotland								
Rhiddoroch (RHD)[b]	–4.98	57.90	180–230	PISY	X	–	X	Rydval et al. (2017b)
Glen Affric (GAN)	–4.92	57.28	300	PISY	X	X	–	Rydval et al. (2017b)
Ryvoan (RYO)[c]	–3.65	57.17	420–480	PISY	X	X	X	Rydval et al. (2017b)
Glen Derry North (GDN)[d]	–3.58	57.05	530–600	PISY	X	–	X	Rydval et al. (2017b)
Quoich (QUO)[e]	–3.52	57.02	430–500	PISY	X	–	X	Rydval et al. (2017b)
Inverey (INV)[f]	–3.52	57.00	500–550	PISY	X	–	X	Rydval et al. (2017b)
Upper Glen Feshie (UGF)	–3.87	56.98	400–520	PISY	X	–	X	Rydval et al. (2017b)
Ballochbuie (BAL)	–3.32	56.97	300–500	PISY	X	X	X	Rydval et al. (2017b)
Meggernie (MEG)	–4.33	56.57	325	PISY	X	–	X	Rydval et al. (2017b)
Glen Falloch (GLF)[g]	–4.65	56.37	160–200	PISY	X	–	X	Rydval et al. (2017b)
Continental Europe								
Dolina Suchej Wody	20.03	49.25	1480	PCAB	X	X	–	Büntgen et al. (2007)
Dolina Mengusovska	20.07	49.15	1450	LADE	X	X	–	Büntgen et al. (2007)
Oetztal	11.02	46.85	1900	PCAB	X	X	–	Esper et al. (2007)
Lötschental	7.85	46.47	2200	LADE	X	X	–	Büntgen et al. (2006)
Val di Sole	10.69	46.42	2250	PICE	X	X	–	Cerrato et al. (2019)
The Pyrenees								
Lac d'Aumer	–0.09	42.51	2400	PIUN	X	X	–	Büntgen et al. (2010)
Sobrestivo	–0.06	42.42	2500	PIUN	X	X	–	Büntgen et al. (2010)
Gerber	–0.59	42.38	2400	PIUN	X	X	–	Büntgen et al. (2010)
Port de Cabus	–1.25	42.32	2450	PIUN	X	X	–	Büntgen et al. (2010)
Eyne	–2.07	42.28	2400	PIUN	X	X	–	Büntgen et al. (2010)

[a] For the site Laanila, a larger number of TRW measurements than MXD measurements are included as the number (15) of TRW measurements otherwise would be insufficient to build a reliable chronology.

[b] For Rhiddoroch (RHD), 7 individual MXBI measurement series were deleted due to several zero values.

[c] For the site Ryvoan (RYO), TRW and MXBI parameters were measured on the same samples. However, MXD was measured on samples from the same trees but not on the exact same sample as TRW and MXBI. The MXD samples were extracted just above where cores for TRW and MXBI were extracted.

[d] For Glen Derry North (GDN), 4 individual MXBI measurement series were deleted due to several zero values.

[e] For Quoich (QUO), 2 individual MXBI measurement series were deleted due to several zero values.

[f] For Inverey (INV), 3 individual MXBI measurement series were deleted due to several zero values.

[g] For Glen Falloch (GLF), 14 individual MXBI measurement series were deleted due to several zero values.

within a window length of 50 years, with a window overlap of 25 years, meaning an EPS value every 25 years from the beginning of the time series to the last year. Table 2 report the minimum and the maximum values of sample depth and EPS from 1860 to 2000. The frequently used, but arbitrarily chosen, EPS threshold of 0.85 suggests that a tree-ring chronology is dominated by a clear population-level signal rather than by individual noise (Speer, 2010).

2.2. Instrumental temperature data

Instrumental data for this study were obtained from HadCRUT4.04 (Morice et al., 2012), consisting of gridded monthly mean temperature data and presented on a 5° latitude by 5° longitude grid. It is a blend of the CRUTEM4 land surface air temperature dataset (Jones et al., 2012) and the HadSST3 sea surface temperature dataset (Kennedy et al., 2011a,b). The temperature data from each meteorological station was first converted to an anomaly with regard to the 1961–90 average temperature for the station and then the monthly mean was calculated for all the station anomalies within each 5°×5° grid-cell from 1850 to the present. We started our analysis in 1860 because of considerable missing data in earlier years (Christiansen and Ljungqvist, 2017) and since the instrumental temperature measurements contain a well-known warm bias during the summer months prior to *c.* 1860 (Moberg et al., 2003; Frank et al., 2007; Böhm et al., 2010).
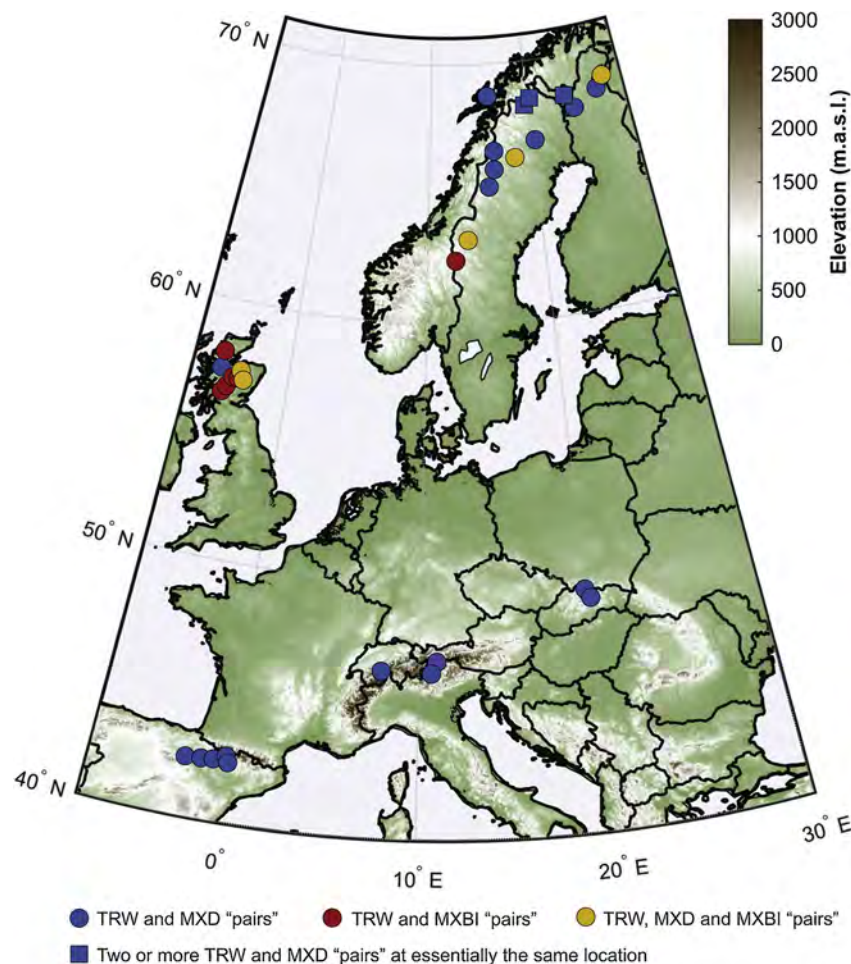
Fig. 1. Map showing the location of the temperature-sensitive tree-ring data. The colour-coded symbols indicate "pairs" of TRW, MXD, and MXBI data. Square symbols indicate two or more TRW and MXD "pairs" from essentially the same location.

The reason we use the HadCRUT4 ensemble of gridded instrumental temperature data, rather than just the land-based part – i.e. CRUTEM4 (Jones et al., 2012) – is to assess the sensitivity of our results to small variations in the instrumental temperature data used. An ensemble, consisting of 100 different members, for this purpose is only available for the HadCRUT4 data set. The 100 ensemble members sample the spread of the possible distribution surface temperature anomalies while considering method-choice biases from station homogenisation adjustment procedures, station climatological normal uncertainties, adjustments for urbanisation, the influence of thermometer exposure biases, and data coverage uncertainties.

Christiansen and Ljungqvist (2017) explored the uncertainties inherent in the HadCRUT4 data set, and their Figure 7 shows that before 1950 most of the uncertainties are represented by the spread of the ensemble, i.e., by systematic errors. It is clear that for the temperatures derived from HadCRUT4 there is a need to in-fill missing values. We therefore inspected all HadCRUT4 local 5°×5° grid-cell series extracted from the data set. It is evident that the 5°×5° grid-cell both for the Pyrenees and for northeastern Scandinavia lack data as noted above, and these years were omitted so that the analysis is performed on the same set of years. The coverage-error in HadCRUT4 decreases with time, becoming small after 1950, but investigating the effect of this on our results is beyond the scope of the present analysis. Sampling and observational errors could additionally be sampled by stochastic modelling, but we will not go further into this issue in the present article.

3. Methods for testing non-linearity

We start with some general considerations regarding linear and non-linear relationships between two variables (e.g., temperature and tree growth). The concept of a linear relationship suggests that two quantities or variables are proportional to each other. The most widely used statistical tool for exploring a linear relationship between variables is the linear regression model: $y = a + bx + e$, where y and x are the respective variables. The variable e captures all other factors which influence the dependent variable y other than the regressor x including noise. Furthermore, a and b are unknown parameters that can be estimated by ordinary least squares (OLS) when we have observations of the variables x and y. This model is a so-called parametric model, as we have specified a functional relationship between the variables x and y, and in this case a linear relationship. However, there are cases where such a model is unsuitable because of intrinsic non-linearity in the data.

One way of accounting for non-linearities is to adjust the linear regression model to a non-linear version: e.g., $y = a + bx^2 + e$. Doubling x now gives rise to a quadrupled increment of y. However, this is still a parametric model since the functional relationship between y and x is specified. Furthermore, we can still use OLS to estimate the unknown parameters, a and b, as we can now transform the data of x by squaring it before applying the estimation method (OLS). However, sometimes we do not know the true functional relationship between x and y, thus we would like to have a method that does not impose a
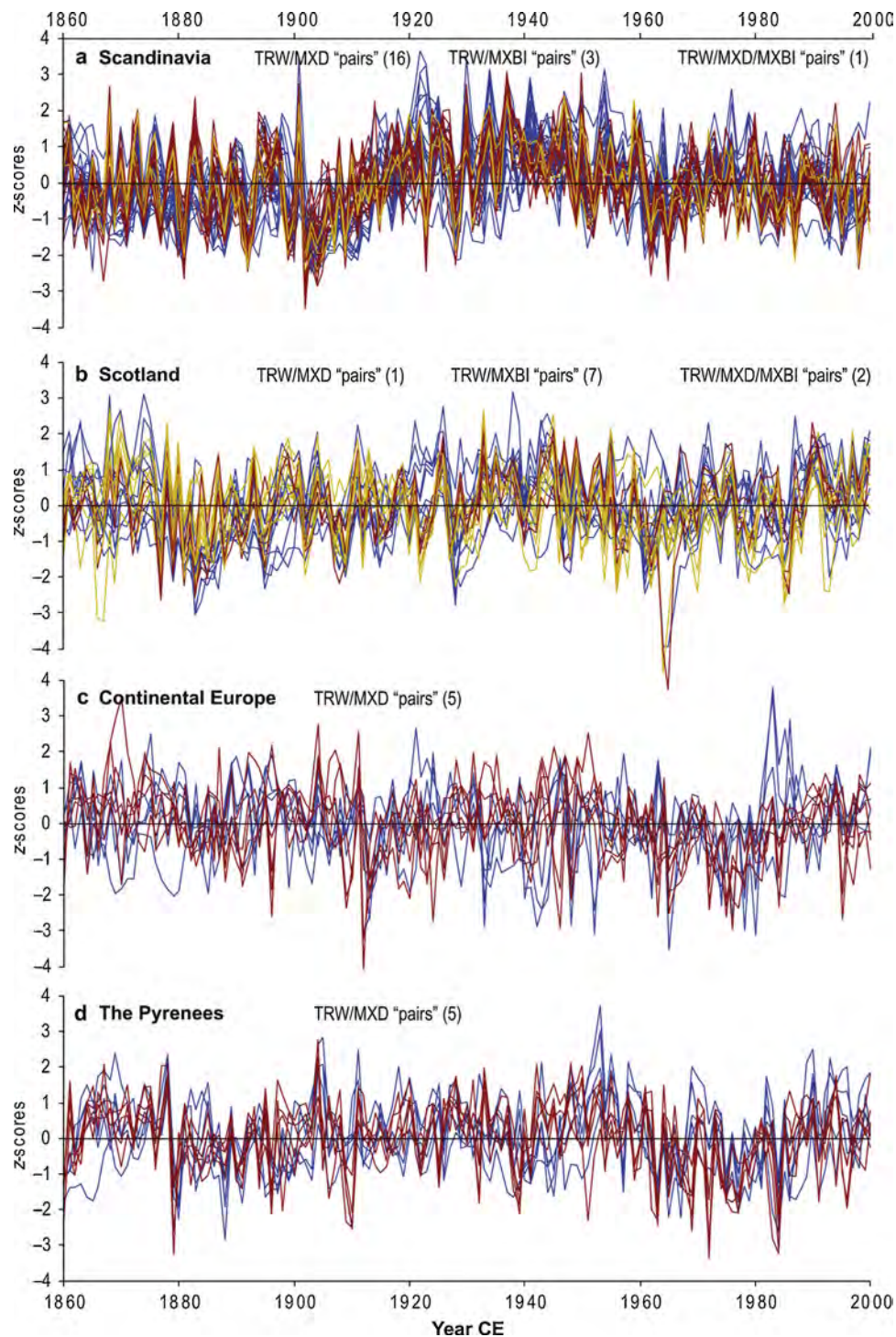
Fig. 2. Visualisation of the included tree-ring data over the period 1860–2000 for each regional subset, standardised to *z*-score units over the full period, with TRW data in blue, MXD data in red, and MXBI data in yellow. (**a**) Scandinavia, (**b**) Scotland, (**c**) Continental Europe, and (**d**) the Pyrenees. Note the overall larger spread in the TRW data and the similarity between MXD and MXBI data. The numbers within the parentheses indicate the number of "pairs".

particular functional relationship. This is possible by using a non-parametric regression model: $y = s(x) + e$, where s is an unknown function that can be estimated by various "smoothing" or kernel methods (Fan and Gijbels, 1996). Such a model is called non-parametric, since we do not assume a specific functional form of s. However, the estimate of s may reveal a non-linear relationship, and the obtained estimate can even guide us to set up a parametric functional form for s, either linear or non-linear, depending on the shape of the estimate of s.

So far, we have only considered a single variable as the regressor x

but the above can be extended to many regressors $x_1, ..., x_p$. However, it is well known that estimation of such high-dimensional problems using non-parametric methods suffers from the so-called curse-of-dimensionality, e.g., that in order to obtain a statistically sound and reliable result in the estimate of s, the amount of data needed to support the result grows exponentially with the dimensionality. Thus, one often assumes additivity, as we also will do throughout this article, i.e. with $p = 2$, $y = a + s_1(x_1) + s_2(x_2) + e$, where again s_1 and s_2 represent unknown functions that must be estimated, typically by the back-fitting

Table 2

Pearson correlation coefficient values (*R*) between instrumental June–August temperature data and tree-ring records and the autocorrelation (AC1) values for tree-ring records included in this study. Abbreviations as follows: MXBI = maximum blue intensity; MXD = maximum latewood density; TRW = tree-ring width; T = Instrumental temperature; EPS = Expressed Population Signal. An EPS value exceeding 0.85 suggests the dominance of a clear population-level growth/climate signal. The sample depth shows the range from the lowest to the highest sample depth occurring during the period 1860–2000. All tree-ring records are listed after latitude from north to south. A dash (–) indicates the absence of data.

Record	R TRW	R MXD	R MXBI	AC1 T	AC1 TRW	AC1 MXD	AC1 MXBI	EPS TRW	EPS MXD	EPS MXBI	Sample depth
Scandinavia											
Northern Finland	0.39	0.68	0.59	0.16	0.86	0.36	0.55	0.95–0.99	0.90–0.95	0.96–0.99	69–84
Forfjorddalen	0.54	0.63	–	0.11	0.50	0.10	–	0.96–0.98	0.97–0.98	–	31–42
Kiruna (KID)	0.49	0.73	–	0.16	0.77	0.20	–	0.98–0.98	0.99–0.99	–	45–101
Kiruna (KIW)	0.46	0.74	–	0.16	0.67	0.32	–	0.96–0.98	0.96–0.98	–	25–83
Ketomella (PTD)	0.38	0.68	–	0.16	0.68	0.20	–	0.97–0.98	0.98–0.99	–	43–58
Ketomella (PTK)	0.33	0.72	–	0.16	0.78	0.35	–	0.96–0.98	0.98–0.99	–	58–69
Ketomella (PTW)	0.34	0.71	–	0.16	0.74	0.36	–	0.96–0.98	0.98–0.99	–	36–39
Torneträsk (TOD)	0.42	0.70	–	0.11	0.70	0.27	–	0.96–0.98	0.98–0.99	–	36–42
Laanila	0.42	0.66	–	0.16	0.64	0.41	–	0.94–0.98	0.93–0.97	–	33–58
Torneträsk (TOD)	0.42	0.70	–	0.11	0.70	0.27	–	0.96–0.98	0.98–0.99	–	33–95
Torneträsk (TOW)	0.47	0.69	–	0.11	0.71	0.28	–	0.94–0.97	0.96–0.98	–	13–77
Kesänkijärvi (KES)	0.25	0.75	–	0.16	0.51	0.07	–	0.97–0.98	0.99–0.99	–	72–86
Luosu (PIS)	0.17	0.67	–	0.16	0.63	0.03	–	0.93–0.98	0.97–0.99	–	26–55
Luosu (PIT)	0.15	0.71	–	0.16	0.65	0.12	–	0.96–0.97	0.98–0.99	–	36–53
Muddus	0.40	0.63	–	0.16	0.55	0.15	–	0.61–0.79	0.74–0.92	–	6–6
Tjeggelvas	0.33	0.59	–	0.11	0.47	0.15	–	0.90–0.95	0.97–0.98	–	34–53
Arjeplog	0.38	0.57	0.58	0.11	0.58	0.30	0.02	0.92–0.95	0.96–0.97	0.96–0.97	32–41
Ammarnäs	0.44	0.64	–	0.11	0.50	0.09	–	0.90–0.96	0.93–0.98	–	24–35
Kittelfjäll	0.29	0.52	–	0.11	0.69	0.20	–	0.88–0.95	0.93–0.94	–	22–36
Jämtland	0.38	0.65	0.71	–0.03	0.55	0.14	0.10	0.90–0.96	0.95–0.97	0.94–0.97	30–37
Rogen	0.55	–	0.79	–0.03	0.27	–	0.00	0.98–0.99	–	0.97–0.98	104–119
Scotland											
Rhiddoroch (RHD)	0.24	–	0.29	0.11	0.58	–	0.54	0.76–0.86	–	0.86–0.92	10–16
Glen Affric (GAN)	0.21	0.53	–	0.11	0.66	0.39	–	0.69–0.78	0.77–0.86	–	11–11
Ryvoan (RYO)	0.30	0.49	0.32	0.11	0.61	0.39	0.45	0.86–0.91	0.86–0.94	0.86–0.92	14–16
Glen Derry North (GDN)	0.43	–	0.59	0.11	0.58	–	0.16	0.87–0.92	–	0.93–0.94	25–27
Quoich (QUO)	0.35	–	0.63	0.11	0.54	–	0.29	0.66–0.84	–	0.87–0.92	15–17
Inverey (INV)	0.28	–	0.53	0.11	0.75	–	0.24	0.81–0.93	–	0.71–0.87	18–19
Upper Glen Feshie (UGF)	0.29	–	0.67	0.11	0.61	–	–0.02	0.95–0.98	–	0.97–0.98	76–89
Ballochbuie (BAL)	0.33	0.55	0.62	0.11	0.68	0.10	0.05	0.82–0.89	0.91–0.94	0.90–0.93	19–21
Glen Falloch (GLF)	0.23	–	0.43	0.11	0.74	–	0.48	0.95–0.98	–	0.93–0.96	79–82
Meggernie (MEG)	0.18	–	0.41	0.11	0.65	–	0.27	0.78–0.91	–	0.74–0.94	11–20
Continental Europe											
Dolina Suchej Wody	0.50	0.56	–	0.33	0.37	0.13	–	0.96–0.98	0.98-0.99	–	43–56
Dolina Mengusowska	0.24	0.47	–	0.33	0.38	0.21	–	0.97–0.99	0.96–0.98	–	34–58
Oetztal	0.32	0.36	–	0.23	0.67	0.08	–	0.93–0.96	0.96–0.98	–	39–45
Lötschental	0.33	0.58	–	0.16	0.41	0.27	–	0.95–0.97	0.96–0.97	–	24–29
Val di Sole	0.33	0.31	–	0.23	0.63	0.27	–	0.82–0.93	0.72–0.83	–	6–12
The Pyrenees											
Lac d'Aumer	0.26	0.49	–	0.14	0.42	0.09	–	0.96–0.98	0.97–0.98	–	50–64
Sobrestivo	0.02	0.03	–	0.14	0.44	0.11	–	0.91–0.93	0.86–0.91	–	26–33
Gerber	0.19	0.32	–	0.14	0.38	0.02	–	0.95–0.98	0.96–0.97	–	62–69
Port de Cabus	0.28	0.38	–	0.14	0.33	0.19	–	0.91–0-94	0.92–0.94	–	17–23
Eyne	0.28	0.39	–	0.14	0.51	0.11	–	0.93–0.97	0.95–0.98	–	32–70

algorithm, confer Section 3.1. The generality of such additive models is attractive. However, precision and power are likely to be lost if a non-parametric component is adopted when a linear or other parametric term is adequate. There are therefore many situations where a semi-parametric approach will be more beneficial. Models of this type allow mixtures of linear and non-parametric components, for example $y = a + b_1 x_1 + s_2(x_2) + e$, where now the variable x_1 is having a linear effect on the response y, whereas the variable x_2 has a non-parametric, thus potentially a non-linear, effect on y due to the estimation of the unknown function s_2.

In this article, we compare four different models – a linear model, two semi-parametric models, and a full non-parametric model – by examining the Akaike Information Criterion (AIC) (Akaike, 1974). AIC is an estimator of the relative quality of statistical models for a given set of data. Given a collection of models for the data, AIC estimates the quality of each model, relative to each of the other models. In this way AIC provides a means for calibration model selection.

3.1. Non- and semi-parametric regression models

As outlined above, non- and semi-parametric modelling aim to relax assumptions about the form of a regression function, by letting the data define a suitable function that describes the available data well. These approaches are powerful in exploring fine structural relationships and provide useful diagnostic tools for parametric models. This leads us to the following additive non-parametric model between observables Y and X,

$$Y = \alpha + \sum_{j=1}^{d} s_j(X_j) + e, \tag{1}$$

where $s_1, ..., s_d$ are unknown (smooth) uni-variate functions, $E(e) = 0$, $\mathrm{Var}(e) = \sigma^2$ and e is independent of the vector of co-variates X. To ensure identifiability, $s_1, ..., s_d$ are required to satisfy

$$E[s_j(X_j)] = 0, \ j = 1, ..., d, \tag{2}$$

which implies that $E(Y) = \alpha$. Estimation of the unknown functions

$s_1, ..., s_d$ can be done by the back-fitting algorithm, introduced by Breiman and Friedman (1985) and Buja et al. (1989). A description of the back-fitting algorithm is available in Støve et al. (2012), along with examples of the implementation of these methods in a palaeoclimate context, and further theoretical details about the methods.

In the linear regression model each regressor represents one degree of freedom – in the additive model more degrees of freedom are used up, see Hastie and Tibshirani (1990), which is detrimental to the statistical power when addressing a fixed amount of data – it is therefore generally advantageous to consider models that contain both linear and non-linear terms using semi-parametric models,

$$Y = \alpha + \sum_{j=1}^{p} s_j(X_j) + \sum_{j=p+1}^{d} \beta_j \cdot X_j + e. \tag{3}$$

3.2. Testing "pairs" of tree-ring data for non-linearity

For "pairs" of tree-ring width (TRW_i) and maximum tree-ring density (MXD_i) (or maximum blue intensity, $MXBI_i$) at a specific location and for year i, regressions for a purely linear model, a purely non-parametric, and two mixed semi-parametric models are performed. Below, MXD is understood to indicate MXD as well as MXBI,

$$T_i = \beta_1 \cdot TRW_i + \beta_2 \cdot MXD_i + \epsilon_i, \tag{4}$$

$$T_i = \beta_3 \cdot TRW_i + s_1(MXD_i) + \epsilon_i, \tag{5}$$

$$T_i = s_2(TRW_i) + \beta_4 \cdot MXD_i + \epsilon_i, \tag{6}$$

and

$$T_i = s_3(TRW_i) + s_4(MXD_i) + \epsilon_i. \tag{7}$$

where T_i is the observed temperature, $\beta_1 - \beta_4$ are unknown parameters, $s_1 - s_4$ unknown smoothing functions, and ϵ i.i.d. error terms.

3.3. Calibration model inter-comparison

We are posing the testable question whether TRW or MXD (or MXBI) is the most linear carrier of temperature information. We do this by testing the four separate regression-style models and comparing their ability to represent temperature at different locations: a fully linear model (Eq. (4)), a fully non-linear model (Eq. (7)), and the semi-parametric models (Eqs. (5) and (6)), where the latter two allow interchange of the roles played by TRW and MXD (MXBI). We use tests based on descriptive statistics for goodness of fit and significance of the fits to answer these questions.[1]

We inspect terms in the full non-linear model (7) for significance of the non-linear terms in order to (a) ensure that the terms, and thus the model, is indeed statistically significant, and (b) whether one term is more significant than the other. Together, the analysis is intended to reveal whether (1) a full non-linear model for both TRW and MXD (MXBI) best utilises the information in the data, (2) whether it is TRW or MXD (MXBI) that is most in need of non-linear treatment – i.e. which one is the most non-linear, and (3) whether the best model is significantly better than the other models.

By performing a relative analysis like this, and doing so for a set of tree-ring "pairs", and using the HadCRUT4 temperature ensemble (Morice et al., 2012) we can derive a distribution of p values and AIC values and directly test for significant differences in the statistics by distribution-comparison, which is a simpler and more intuitive way of testing a set of results than is e.g. Bonferroni-corrections (Bonferroni, 1936), or other methods, e.g. Dunn (1961) used when analysing joint significance levels. By counting the number of cases in which AIC for

---

[1] All coding was performed using the software environment R (Core Team, 2018) and in particular the GAM library (Wood, 2017).

the model with TRW treated as non-linear was smaller than the number of cases where AIC for the model where MXD (MXBI) was treated as non-linear, we can use the "sign test" (Arbuthnott, 1710; Dixon and Mood, 1946) to express the probability that the observed counts could be drawn from a simple null hypothesis along the lines of "either outcome is equally likely".

We use the standard 0.95 probability level throughout the study. That choice will be made explicit in the following sections; however, it can be briefly summarised by the following: Comparisons of AIC values are based on finding which of several model-fits obtained the smallest AIC value. The best model is that with the smallest AIC value – either smallest positive number or most negative number. However, when two AIC values do not differ by much there is not so much relevance in the test. As AIC values are similar to likelihood ratios it is possible to explicitly state that an AIC-difference between two compared model fits (with the same number of parameters), that differ by more than ≈ 6, indicates that the model-fit with the smaller AIC is significantly better, at the standard p level of 0.95. We use the simple sign test to express the significance of the distribution based on the 100 ensemble members: e.g., if 95 of the 100 ensemble members show the same result – i.e. that either TRW or MXD (MXBI) is the more non-linear parameter – we use this count as the indicator of significance.

4. Results

4.1. Correlation and autocorrelation structure

Both MXD and MXBI data exhibit a considerably stronger correlation with instrumental June–August temperature than TRW data (Fig. 3a): the mean/median correlation R is 0.33/0.33 for TRW, 0.57/0.61 for MXD, and 0.57/0.59 for MXBI. The first and third quartiles of the distribution of correlations between TRW data and temperature do not even overlap with the first and third quartiles of the distribution of correlations between temperature and MXD (MXBI) data. Notably, the correlation strength is close to identical for MXD and MXBI data.

The correlation between TRW and MXD (MXBI) data from the same sites over the period 1860–2000 are relatively high: mean/median R for TRW/MXD is 0.51/0.55 and for TRW/MXBI 0.54/0.58 (Fig. 3b). The mean/median correlation between MXD/MXBI series, bearing in mind that we only have five MXD and MXBI records from the same sites (Table 1; Fig. 1), is as high as 0.89/0.91. Considering the almost identical correlation between TRW/MXD and TRW/MXBI series, together with the extremely high MXD/MXBI correlation, we may conclude that MXD and MXBI data exhibit almost identical characteristics (at least in the studied frequencies).

The autocorrelation is much higher for TRW data than for either instrumental June–August temperature data (here represented by the local 5°×5° grid-cells corresponding to tree-ring locations) or for MXD or MXBI data (Fig. 3c). The mean/median instrumental autocorrelation is 0.13/0.13, for MXD data 0.20/0.19, for MXBI data 0.24/0.24, and for TRW 0.58/0.60. As with the case of the correlation to instrumental data, the first and third quartiles for the autocorrelation values for TRW do not even overlap with the first and third quartiles for the autocorrelation values for MXD/MXBI data. On the other hand, the first and third quartiles for the autocorrelation in instrumental data are fully overlapping with the first and third quartiles for the autocorrelation for MXD/MXBI data.

A tendency to a negative relationship between correlation strength and autocorrelation can be observed for TRW data from each of the four regions (Scandinavia, Scotland, Continental Europe, and the Pyrenees). It means that TRW records with a stronger correlation to instrumental temperature data, in general, have a lower autocorrelation than those records with a weaker correlation to instrumental temperature. No relationship can be found for MXD data between correlation strength and autocorrelation. MXBI records with a low autocorrelation (i.e., similar to instrumental autocorrelation) also show higher correlation values.
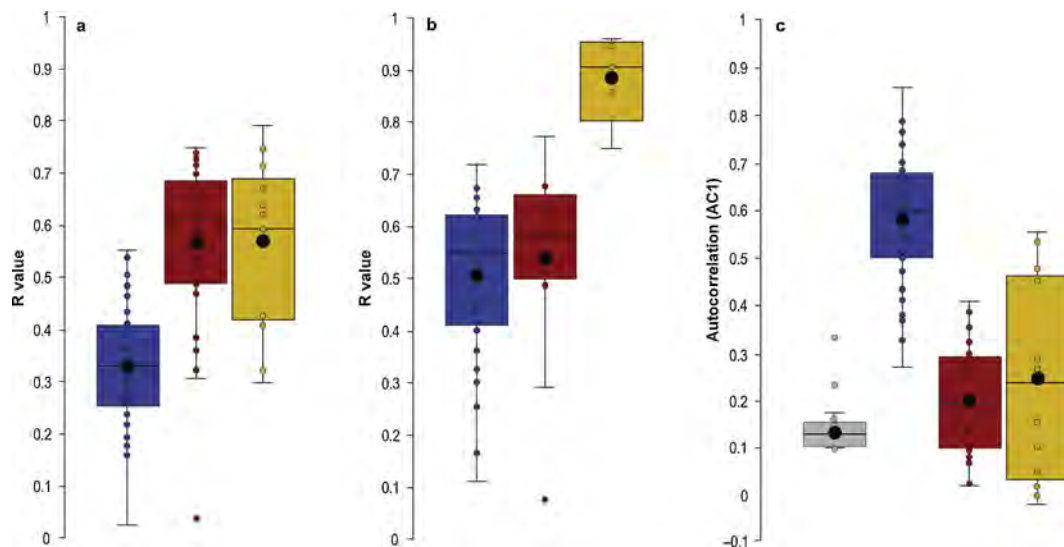
Fig. 3. Box-plot figures showing (**a**) the Pearson correlation coefficient (*R*) between instrumental June–August temperature data and TRW (blue), MXD (red), and MXBI (yellow) data over the period 1860–2000, (**b**) Pearson correlation coefficient (*R*) between TRW and MXD (blue), TRW and MXBI (red), and MXD and MXBI (yellow) data over the period 1860–2000, and (**c**) the autocorrelation (AC1) value for June–August instrumental temperature data from 5°×5° grid-cells corresponding tree-ring record locations (grey), TRW (blue), MXD (red), and MXBI (yellow) data over the period 1860–2000. The coloured bars represent the first and third quartiles, the line across the box shows the median, the black dot is the mean, the filled circles represent each individual value, and minimum and maximum values are indicated by the whiskers.

4.2. Linear and non-linear temperature response

Tables 3 and 4 presents summary statistics of the four regressions in Eqs. (4)–(7). Eq. (4) is the fully linear model – we allow both TRW and MXD (MXBI) to be in the regression model as linear terms; Eq. (7) is the fully non-linear model – i.e., we allow both TRW and MXD (MXBI) to be represented as non-linear terms in the regression, which allows for capture of non-linear behaviour; Eqs. (5) and (6) are the pair of models that only allow either TRW or MXD (MXBI) to be treated as linear while the other is treated as non-linear. Comparison of the successes of these last two models is the key to our analysis: by looking at the results for these two models, we find out whether TRW or MXD (MXBI) are best represented as non-linear relative to the other model, i.e., whether TRW or MXD (MXBI) best capture temperature information linearly or non-linearly.

Tables 3 and 4 shows the AIC values for each model. These statistics are based on the medians of the samples of values obtained by fitting models to each version of the HadCRUT4 ensemble. In the last column of Tables 3 and 4 we show results pertaining to the performance of individual members of this ensemble. This ensemble consists of 100 equally realistic versions of HadCRUT4 temperature ensemble members for the given 5°×5° grid-cell locations, given processing steps in generating the HadCRUT4 series from "raw" temperature observations and taking realistic observing choices and uncertainties into account (see Section 2.2).

Inspecting the medians of the AIC values of the four models over the instrumental temperature ensemble (the 4 columns following the tree-ring record name) we see that AIC for the fully non-linear model performs best for 31 of the 32 records with two ties, and one performs less well (the record Luosu [PIS]). Comparing only the two semi-parametric models, we find that the model where TRW is treated non-linearly and MXD linearly always performs best, except for two records – Ketomella (PTW) and Oetztal – for which model (5) (i.e. MXD is treated as non-linear and TRW as linear) shows higher skill. However, small differences in AIC (say, less than 6) are not significant at the p_{crit} = 0.05 level on an individual basis. We note that between the two semi-parametric models (Eqs. (5) and (6)) we have only 4 cases (Northern Finland, Luosu [PIS], Glen Affric [GAN], and Dolina Mengusowska) where one shows better AIC results than the other by as much as 5. However, these

AIC values are based on distribution medians.

Considering the *individual* performances over the instrumental June–August temperature ensemble of 100 realisations for each 5°×5° grid-cell (last column of Tables 3 and 4) we note that for 16 "pairs" of TRW *vs.* MXD data (out of the 32 "pairs") AIC for model (6) (i.e. where TRW is treated as non-linear and MXD as linear) is smaller (i.e. better) than AIC for model (5) (i.e. MXD is treated as non-linear and TRW as linear) across more than 95% of the ensemble, and for 28 records in more than 50% of the ensemble. This joint result is a robust indicator that the model in Eq. (6) (i.e. where TRW is treated as non-linear and MXD as linear) is better at explaining variance than the model in Equation (5) (i.e., MXD as non-linear and TRW as linear) for most records and for most temperature ensemble members. The model in Eq. (6) contains smoothing of TRW, and we interpret this as TRW having a more non-linear relationship to instrumental temperature data than MXD data.

Considering TRW *vs.* MXBI we find that out of 13 MXBI records tested, the model treating TRW and MXBI *both* as non-linear performs best in 12 cases with one tie (Rogen is the exception). Comparing the two mixed models (TRW treated as linear and MXBI treated as non-linear *vs.* TRW treated as non-linear and MXBI treated as linear) we find an almost equal split – 6 of the 13 records are best treated with TRW as a linear term, while for 7 records it is better to treat MXBI as the linear term and TRW as the non-linear term. Looking at the performance of individual ensemble members (i.e. looking at column *N* in Tables 3 and 4) we find that 6 of the 13 records favour treating TRW as non-linear at the 95% significance level – however, these are also the only records performing better at the 50% level, unlike Table 3 where TRW *vs.* MXD was compared. The results for TRW *vs.* MXBI are thus not like those for TRW *vs.* MXD – for "pairs" of TRW and MXBI there is an almost even split between favouring TRW as non-linear, or MXBI.

In summary, we observed (see also Fig. 4) a robust and strong tendency for most TRW series to be best represented as non-linear terms in the temperature-models, compared to MXD, although exceptions to this exist in individual cases. However, for TRW *vs.* MXBI (Fig. 4 b and c) no such strong tendency is seen, although pure linear treatment for both TRW and MXBI is ruled out by our results. We discuss possible reasons for these exceptions, and the difference between MXD and MXBI data, in Section 5.3.

Table 3

Non-linearity testing using GAM models based on "pairs" of TRW and MXD data. Equations (4)–(7) were fitted to local 5°×5° grid-cell June–August temperature data from HadCRUT4.0 (Morice et al., 2012). At each location the full HadCRUT4 temperature data ensemble (100 members) was fitted one at a time and then the ensemble-median values of statistical quantities were calculated and shown here. The first column contains the names of the tree-ring records. Columns 2–5 represent AIC values for the full linear model, the two mixed models, and the full non-linear model, respectively. The column labelled AICmix1 gives the AIC value for the model in Eq. (5) treating MXD as the non-linear term. The column labelled AICmix2 gives the AIC value for the model in Eq. (6) treating TRW as the non-linear term. Columns AIClm and AICgam represent the fully linear and the fully non-linear models. The last column, labelled N, shows results of individual model-comparisons across the 100 ensemble members. The value given is the number (N), out of 100 ensemble trials, where the model (6) had smaller AIC than the model (5) – that is, when the analysis indicates that model performance benefits from treating TRW rather than MXD as non-linear. Values in bold indicate p-values of 0.05 using a simple sign test (Dixon and Mood, 1946). All tree-ring records are listed after latitude from north to south.

Record	AIClm	AICmix1	AICmix2	AICgam	N
Scandinavia					
Northern Finland	283.86	283.85	275.83	275.83	**100**
Forfjorddalen	333.07	333.04	332.84	332.45	**74**
Kiruna (KID)	298.59	298.58	298.39	298.14	42
Kiruna (KIW)	297.46	297.43	295.80	295.57	**87**
Ketomella (PTD)	321.38	321.37	320.55	320.50	**99**
Ketomella (PTK)	302.13	302.12	301.78	301.60	31
Ketomella (PTW)	303.02	300.93	302.55	300.87	5
Laanila	291.78	290.50	289.93	288.58	**88**
Torneträsk (TOD)	314.17	314.15	313.02	312.99	**97**
Torneträsk (TOW)	312.03	311.87	311.15	311.08	**94**
Kesänkijärvi (KES)	293.10	293.04	291.46	291.31	**93**
Luosu (PIS)	321.22	320.80	315.23	315.23	**100**
Luosu (PIT)	310.08	310.08	309.41	309.38	**100**
Muddus	334.70	334.60	334.01	333.90	**95**
Tjeggelvas	346.30	346.29	344.84	344.83	**100**
Arjeplog	350.61	350.58	349.81	349.66	**100**
Ammarnäs	332.68	332.63	332.39	332.17	69
Kittelfjäll	363.07	363.04	361.61	361.60	**100**
Jämtland	332.96	332.48	330.99	330.93	**93**
Scotland					
Glen Affric (GAN)	359.61	359.59	354.25	354.19	**100**
Ryvoan (RYO)	368.56	360.51	357.41	356.88	**100**
Ballochbuie (BAL)	357.17	356.72	356.41	356.01	**70**
Continental Europe					
Dolina Suchej Wody	327.46	327.44	327.43	327.39	**91**
Dolina Mengusowska	370.40	355.79	345.95	345.90	**100**
Oetztal	376.20	375.78	376.05	375.40	24
Lötschental	350.20	349.67	348.21	347.65	**99**
Val di Sole	385.83	385.52	383.07	382.52	**100**
The Pyrenees					
Lac d'Aumer	368.25	368.12	364.82	363.97	**99**
Sobrestivo	406.85	405.05	404.97	403.14	59
Gerber	391.69	391.59	390.46	390.52	**92**
Port de Cabus	381.24	381.17	377.14	376.97	**100**
Eyne	379.29	379.23	379.04	378.97	**90**

4.3. Relationships between non-linearity, correlation strength and autocorrelation

We find no consistent patterns between non-linearity and correlation strength or autocorrelation structure. Even though we only evaluate 40 sites, divided into four regions with different climate-dependent data properties, the absence of a pattern can be interpreted at least in qualitative terms. Neither correlation strength nor autocorrelation of either TRW or MXD (MXBI) data stands out in the cases where TRW data show a more linear response to temperature in the majority of the cases that are evaluated using the HadCRUT4 instrumental temperature ensemble.

Special consideration may be given the only two records – Ketomella (PTW) and Oetztal – where a higher skill is obtained by

Table 4

Non-linearity testing with GAM modelling using "pairs" of TRW and MXBI data (instead of "pairs" of TRW and MXD data). For reference, the column labelled AICmix1 gives the AIC value for the model in Eq. (5) which is the model treating MXD as the non-linear term. The column labelled AICmix2 gives the AIC value for the model in Eq. (6) which is the model treating TRW as the non-linear term. Columns AIClm and AICgam represent the fully linear and the fully non-linear models. The last column N shows the number of times, out of 100, that the temperature ensemble reveals a more non-linear relationship between temperature and TRW data than between temperature and MXBI data. Values in bold indicate p-value of 0.05 using a simple sign test (Dixon and Mood, 1946). All tree-ring records are listed after latitude from north to south.

Record	AIClm	AICmix1	AICmix2	AICgam	N
Scandinavia					
Rogen	272.70	272.78	270.80	272.42	**96**
Arjeplog	348.14	348.11	347.74	347.63	**100**
Northern Finland	308.93	308.91	303.53	303.52	**100**
Jämtland	311.14	311.01	309.76	309.71	**96**
Scotland					
Ballochbuie (BAL)	340.60	338.13	339.71	337.29	0
Ryvoan (RYO)	389.30	333.55	369.42	332.31	0
Glen Falloch (GLF)	374.69	374.66	373.52	372.96	**100**
Glen Derry North (GDN)	348.20	346.09	346.80	344.44	18
Inverey (INV)	358.23	357.44	358.04	357.28	9
Meggernie (MEG)	376.96	373.93	374.03	371.28	46
Quoich (QUO)	334.98	334.96	333.40	333.40	**100**
Rhiddoroch (RHD)	393.54	382.82	392.88	382.33	0
Upper Glen Feshie (UGF)	325.09	321.56	323.98	320.59	0

treating MXD as a non-linear term and TRW as a linear term. Ketomella (PTW) has an unusually high autocorrelation for MXD data, although not higher than for a few other MXD records that also show a more linear response to temperature than TRW data from corresponding sites. For Oetztal, the correlation values are relatively low for both TRW and MXD, and the MXD data show a significantly *lower* autocorrelation than the instrumental data; moreover, an inverse relationship during certain years is detected in the TRW and MXD data.

Most of the Scottish tree-ring series show a low or relatively low inter-series correlation (see Section 2). This may contribute to a spurious detection of non-linearity among many of the Scottish series. Diverging trends between TRW and MXBI data appears to be a plausible reason why many MXBI records from Scotland are showing a more non-linear response to temperature than the TRW records from corresponding sites. The two MXBI records from Scotland showing a consistently more linear response to temperature than the TRW records from the same sites – Glen Falloch (GLF) and Quoich (QUO) – have stable (or slightly increasing) MXBI values and increasing TRW in the post-1980 period. For Ballochbuie (BAL), Inverey (INV), Ryvoan (RYO), and Upper Glen Feshie (UGF) the MXBI values are stable since the 1980s whereas the TRW values are increasing; for Meggernie (MEG) and Rhiddoroch (RHD) the MXBI values are stable since the 1950s whereas the TRW values are decreasing. The MXD values for Ballochbuie (BAL) and Ryvoan (RYO) are not behaving as the MXBI values but rather follow the TRW trends.

4.4. Identifying the nature of the non-linearities: two examples

What does it mean that we have found non-linearity in some of the tree-ring proxy series? As an example, we consider the series from Jämtland (Björklund et al., 2014; Linderholm and Gunnarson, 2019). Fig. 5 (upper right-hand panel) shows that of TRW, MXD and MXBI, it is only MXD data that tests positively for non-linearity. We also see that the non-linearity may chiefly be related to low values in the series. As a test we remove those points, and re-apply the GAM procedure, in order to better understand whether they represent a true non-linear response in the tree's physiological system to environmental conditions, or might be "noise".
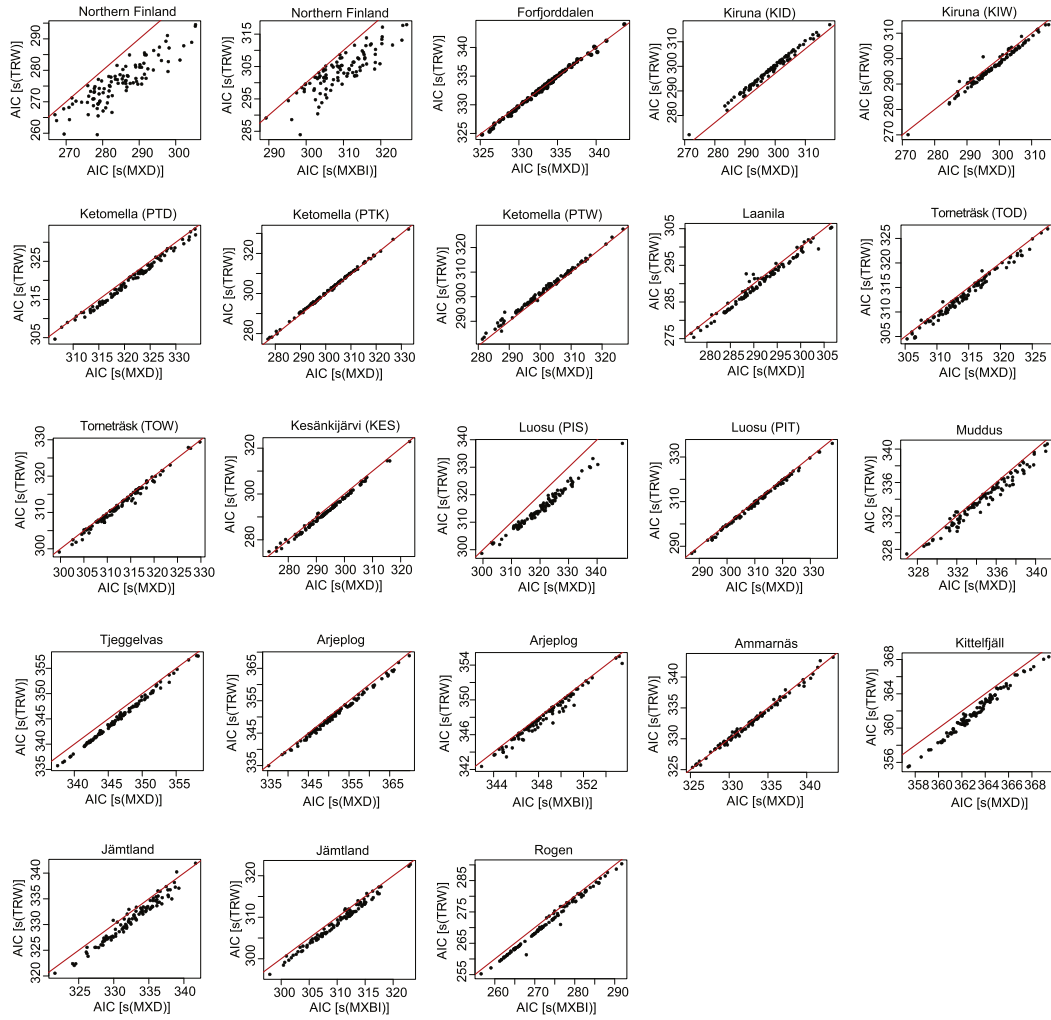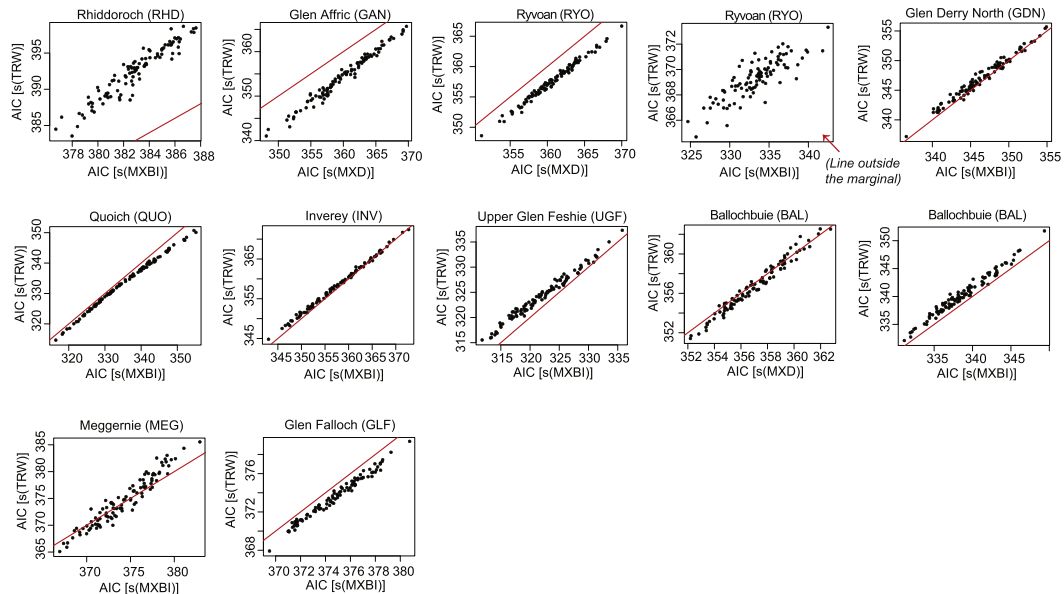
Fig. 4. AIC from the two semi-parametric models fitted to the 100 ensemble members. Each dot represents an AIC-pair for one ensemble member. Ensembles below the red diagonal imply support for TRW as the most non-linear of the two proxies.
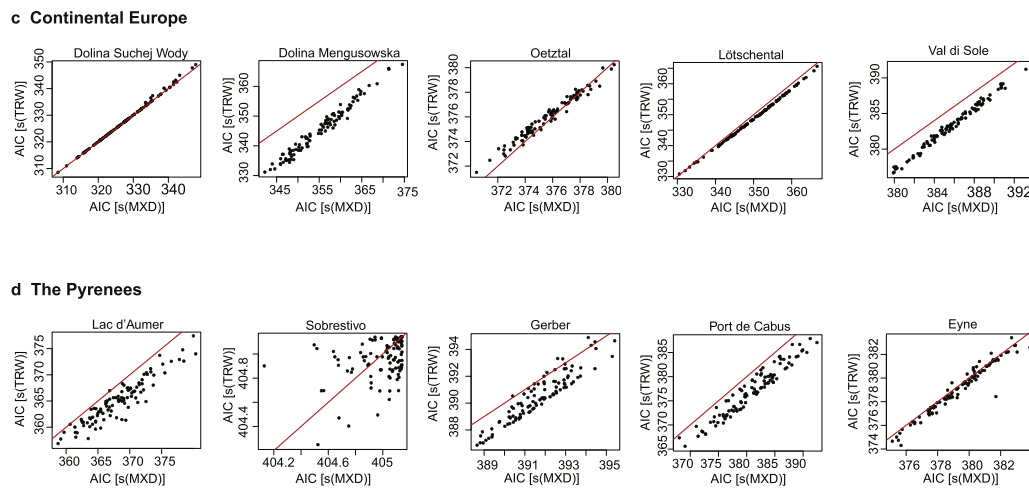
c Continental Europe

d The Pyrenees

Fig. 4. (*continued*)

We inspected the MXD data series and identify the years that correspond to these low values of MXD. We removed increasing number of them (first one then two, …, 18) starting at the smallest value and re-applied the GAM methodology as described above for each set of data. The GAM procedure still detected non-linearity when up to 8 of the smallest values had been removed – but at 9 or more removals linearity was instead detected. This suggests that the non-linearity property is robust – i.e. non-linearity is a property contributed by a substantial fraction of the data. Adding to robustness is also the observation that these MXD values are distributed across the whole time-range of the series – i.e. the low MXD values observed represent a non-linear state of the tree's response to growth conditions, it is not likely a "noise" or "bad data" occurrence.

We also investigated Ballochbuie (BAL) (Rydval et al., 2017b) to see if the nature of the detected non-linearity can be clarified. We subjected the "bulge" (see Fig. 5, lower panels) from – 1 to 0 in standardised TRW data to varying degrees of point removal. The results are more difficult to interpret – partially because the range of data omitted are intermediary to the rest of the data range, and not at the end, as was the case for Jämtland. Removing data values falling between – 0.75 and – 0.25, in standardised TRW data, results in loss of sensitivity in TRW for both the TRW *vs.* MXD and the TRW *vs.* MXBI, with MXD and MXBI becoming approximately linear in both cases. Again, the years affected are not isolated, but are distributed across the range of years, so we are not seeing a "bad data" issue.

5. Discussion

It is, in general, more advisable to use only a smaller number of proxy records with a high temperature correlation strength than to use a larger number of proxy records, when many have a low temperature correlation strength, in large-scale temperature reconstructions (Christiansen and Ljungqvist, 2017) considering the large spatial co-variability of temperature on seasonal and longer time-scales (Jones et al., 1997). This implies that TRW data – with its more non-linear response to temperature, lower temperature correlation strength, and higher autocorrelation – should be avoided whenever a sufficient number of MXD and/or MXBI records are available (see also Esper et al. (2018)). However, for much of the world – and in particular a millennium back in time – very few MXD (and no MXBI) records are available to date (Esper et al., 2016). This is essentially precluding such a selective approach for tree-ring based millennium-long temperature reconstructions on continental to hemispheric scales (see, however, Schneider et al. (2015)). Under these circumstances, our results indicate that any large-scale reconstruction including both TRW and MXD (MXBI) data would benefit from applying a calibration model that treats TRW data non-parametrically (non-linearly) and MXD and MXBI data parametrically (linearly).

5.1. The effect of sample replication and choice of detrending method

The correlation values we show between instrumental temperature data and MXD, MXBI, and TRW data are slightly biased towards low values for TRW when compared to the typical correlation values between temperature and TRW data in published TRW-based temperature reconstructions. This is a result of including fewer TRW samples in the TRW chronologies than is usually the case because we only used the exact same tree-rings, from the same trees, for TRW, MXD and MXBI. Far more tree-ring samples are usually included in a TRW chronology than in a MXD or MXBI chronology as this proxy is comparatively cheap to produce and the large number of samples, given the lower temperature correlation strength in TRW, generally improves the signal as non-climatic noise is cancelled out. To a lesser extent, we also show a bias towards low correlation values for MXD and MXBI as composites of site reconstructions from more locations are typically included in published MXD or MXBI based temperature reconstructions, cancelling out noise and enhancing the temperature signal. An example may be given: calibrating the Torneträsk TRW and MXD records by Melvin et al. (2013) against the same instrumental data as we use gives R 0.53 and R 0.77, respectively, compared to our two sites from Torneträsk, TOD and TOW, giving R 0.42/0.70 and R 0.47/0.69, respectively.

It cannot be precluded (Cook et al., 1995) that some amount of low-frequency information is lost using individual spline detrending (Cook and Peters, 1981, 1997) even if we only consider a comparatively short time-scale of 141 years (1860–2000). However, we have compared ten northern Scandinavian TRW and MXD "pairs" in Büntgen et al. (2011), using both individual detrended chronologies and RCS detrended versions, and found that over 1860–2000 the individual detrended and the RCS detrended chronologies are virtually identical even in their long-term trends. We thus conclude that detrending choices likely have a marginal effect on the results of this study (see further Klippel et al. (2019) regarding the effect of different choices of tree-ring data detrending over various time-scales).

5.2. Sensitivity to seasonality and the length of the calibration period

We may expect the relationship between tree-ring growth and temperature to be more non-linear during certain seasonal windows than during other seasonal windows and that this varies with location (i.e., with climate). The method by Støve et al. (2012) for detecting non-linearity require us to use "pairs" of data, to compare which record of the two behaves in a *more* non-linear way than the other, for the
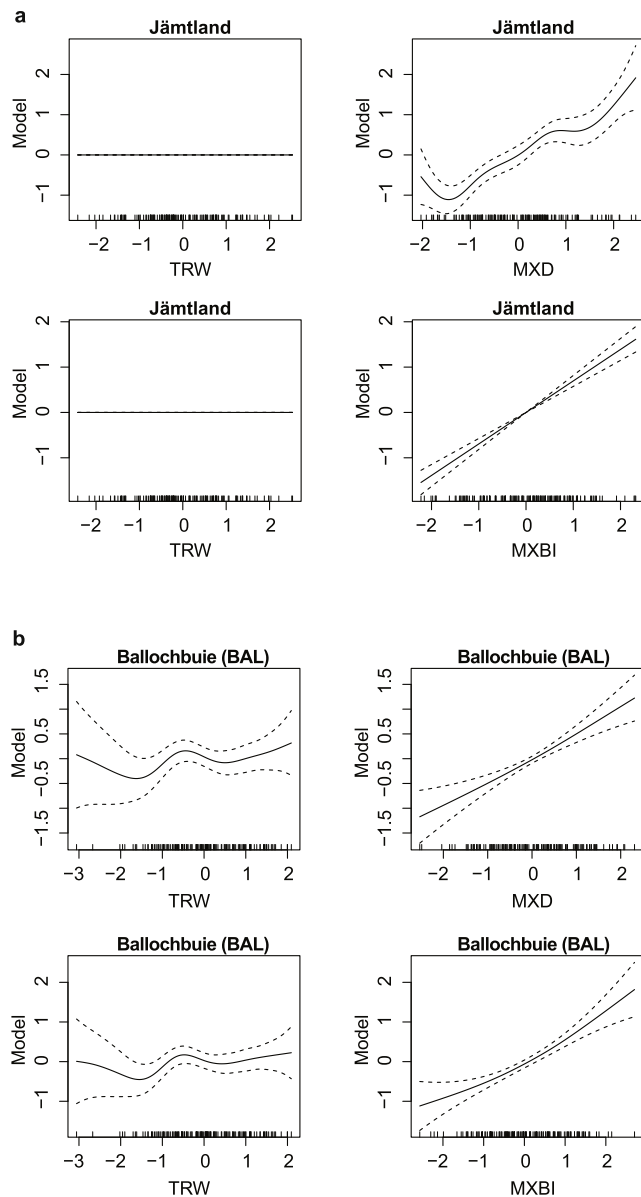
Fig. 5. Example illustration of GAM output. Two full GAM models are shown – one with TRW and MXD as regressors (upper row), and one with TRW and MXBI as regressors (lower row). In the figures, the *x*-axis shows the (standardised) tree-ring values, and on the *y*-axis the instrumental temperature model (also standardised, i.e. unitless) determined by the GAM procedure – where the output may be linear or non-linear. A perfectly horizontal line indicates that no relevant relationship (whether linear or not) has been found between tree-ring values and temperature. A straight diagonal line indicates that a linear relationship has been found, and a curved graph indicates a non-linear relationship. (**a**) Illustration of GAM results for Jämtland (Björklund et al., 2014; Linderholm and Gunnarson, 2019). Note that although TRW by itself may be a relevant regressor in Jämtland it is not detected here when tested in a pair with other regressors – MXD, although found non-linear, manages to also contain the linear dependency. With MXBI no non-linearity at all is detected by the GAM procedure and all the linearity is expressed in MXBI. (**b**) Illustration of GAM results for Ballochbuie (BAL) (Rydval et al., 2017b). When the non-linearity is stronger, or present in both TRW and either MXD or MXBI then GAM finds a non-linear model for both, as in the case with Ballochbuie (BAL). Here, MXD and MXBI both have modest non-linearities but as they are curves and not straight lines GAM formally determined that they are non-linear records. TRW, however, both when paired with MXD and with MXBI, is a much more non-linear proxy. Notice that the models based on TRW depend on which other proxy it was paired with, so in principle the output models for both regressors should be inspected – the case of TRW in Jämtland does not hold in general.

same target season (e.g. June–August) for both TRW, MXD, and MXBI data. It is a plausible hypothesis that *part* of the reason that TRW data behave non-linearly than MXD/MXBI data is related to the much shorter seasonal response window of TRW, which varies with location and tree species (Björklund et al., 2017). We attempted to test for this possibility by repeating all the calculations using the shorter seasonal window of June–July (instead of June–August). At the same time, we note that two metrics with different seasonal response windows can never be fully comparable regardless of which window is chosen. The correlation between TRW and instrumental temperature data increases (but in most cases only marginally) with the seasonal window June–July in 17 out of 40 cases but actually decreases in the other cases. Thus, no general benefit is apparent from using June–July instead of June–August as a calibration target season. As expected, the correlation between instrumental temperature and MXD data *decreases* when using June–July instead of June–August in all cases except one as well as in all cases for MXBI. The mean/median correlation *R* for June–July, compared to June–August, is 0.33/0.34 *vs.* 0.33/0.33 for TRW, 0.47/0.52 *vs.* 0.57/0.61 for MXD, and 0.46/0.50 *vs.* 0.57/0.59 for MXBI data. From this we conclude that June–August (as commonly used) is, in general, a more suitable calibration target season than June–July for MXD and MXBI data, and just as suitable for TRW data.

The choice of a shorter June–July season also has only a modest influence on the AIC values. However, for "pairs" of TRW and MXD data, MXD show a more linear response to temperature than TRW data in a larger number of temperature ensemble members in 12 cases compared to a lower number of temperature ensemble members in 8 cases (this is most clear for data from Scandinavia with the numbers being 10 *vs.* 2). Thus, our main conclusion that MXD data show a more linear response to temperature than TRW data is further strengthened when using the shorter June–July seasonal window. On the other hand, no clearer picture emerges when testing the June–July season, instead of June–August season, on "pairs" of TRW and MXBI data.

5.3. Possible biases in MXD and MXBI measurements

Here we consider two different types of biases, the first arise in the measurement phase and the second is an inherent part of the tree growth. It is possible that, in some cases, limitations associated with MXD or MXBI measurement generation can be responsible for producing MXD or MXBI data that exhibit data non-linearity to a similar degree to TRW. The MXD parameter is commonly obtained from a measurement profile produced by moving a photo sensor across an X-ray image of a tree-ring sample (Schweingruber et al., 1978). With the exception of systems that identify the darkest/most dense parts of a tree ring within a specified window covering a larger area of the latewood of each ring (Rydval et al., 2014), the MXD and MXBI parameters are usually a representation of one or two tracheids in the radial direction (pith to bark) (Vaganov et al., 2006; Campbell et al., 2011). The radial extension of a conifer tracheid in the latewood is typically ≤10 µm, which means that if this spatial resolution is not captured in the measurement profile, the true MXD or MXBI risk being distorted by cells of lower density adjacent to the "true" MXD cells. While the nominal measurement resolution is often defined at ≤10 µm, it can be compromised for several reasons (Björklund et al., 2019) and consequently produce a measurement profile with a deflated amplitude. This translates to a lower mean of all MXD values in a sample, but the MXD measurements of narrow tree-rings also become more deflated than those of wide tree rings. Thus, an artificially strong relationship between TRW and MXD is created. If we expect TRW to be more non-linearly related to a temperature target, MXD or MXBI measured at low resolution could risk being identified as non-linearly related to temperature as well.

Another likely factor that could affect MXBI data is the heart-wood–sapwood discolouration bias (Björklund et al., 2014; Rydval et al., 2014). Rydval et al. (2014) showed that un-detrended versions of

the Scottish MXBI chronologies from Ballochbuie (BAL) and Ryvoan (RYO) exhibit a trend deviation from their MXD counterparts and attributed this discrepancy to a difference in colour between the heartwood and sapwood. Although varying resin extraction approaches (acetone *vs.* ethanol) and measurement systems (CooRecorder *vs.* WinDendro) were used to generate Scottish and Scandinavian MXBI data, respectively, a comparison of the MXBI chronologies produced for the BAL and RYO Scottish sites using a range approaches did not yield appreciably different results and all versions have been shown to contain the same trends which diverge from the MXD chronologies regardless of the methodological approach adopted. Therefore, we do not believe that differences in sample preparation or used measurement systems would account for the non-linear properties of MXBI data from Scotland compared to the Scandinavian data. Instead, it is possible that a greater inherent degree of heartwood–sapwood colour difference between Scottish and Scandinavian MXBI samples may be responsible. Recently developed techniques to correct for discolouration in BI series could potentially be used to remedy this issue (Björklund et al., 2014, 2015) (see Appendix A for further information).

In addition to the above-mentioned measurement bias, some non-linearities could potentially arise from the presence of non-climatic (i.e. disturbance) pulses in the TRW, which could also affect the MXD and MXBI data. This bias is reportedly severe for some of the Scotland data (Rydval et al., 2016), but may also occur in other localities. Although this type of non-climatic impact has not directly been observed to affect MXD or MXBI data, it is, however, not entirely clear whether or not this type of data could also be impacted in some way. The disturbance impact should be thought of as occurring along a continuum where the degree of disturbance affecting a chronology is related to the proportion of samples in a chronology that contain disturbance trends, their severity, and synchronisation. Moreover, the amount of disturbance impact also varies through time meaning that some parts of chronologies may be affected while others are not (or not as much). Observe that only those Scottish chronologies for which the disturbance effect was found to be minimal was retained for the current study (see Section 2.1).

6. Conclusion and outlook

We have systematically compared the presence of a non-linear response to the temperature correlation strength, and the autocorrelation structure in a European network of summer temperature-sensitive TRW, MXD, and MXBI data derived from identical tree-ring samples from 40 different sites. The main findings of this study can be summarised in the following points: (a) The temperature correlation strength is consistently significantly weaker for TRW data than for MXD/MXBI data, while the autocorrelation is much higher for TRW: the distributions of correlation and autocorrelation values hardly overlap with those of MXD/MXBI data. (b) MXD and MXBI data have virtually identical characteristics in terms of non-linearity, temperature correlation strength, and autocorrelation, supporting the view that MXBI is an excellent surrogate for MXD. (c) When TRW and MXD/MXBI data are used in combination, it is advisable to treat TRW as a non-linear function and MXD/MXBI as a linear function.

To validate these findings, we envision that a similar assessment across other regions containing "pairs" of temperature-sensitive tree-ring width and density data would be beneficial. It appears less feasible to follow the "protocol" of this study for hydroclimate-sensitive tree-ring data of the simple reason that very few hydroclimate-sensitive density records have been produced so far. Furthermore, we suggest that our non-linearity test can be applied as an independent and useful tool in dendroclimatology, in that it reveals relationships not otherwise revealed by the standard statistics in dendroclimatology (e.g., EPS values) or tests based on time-series correlations, as discussed in this article.

Appendix A. Tree-ring maximum blue intensity (MXBI) data

As the MXBI parameter may be less well known to many readers, compared to TRW and MXD, we provide a more in-depth description of it here. Blue intensity (BI), also sometimes termed blue reflectance, is a comparatively new, less labour-intensive and less expensive, alternative to MXD with very similar properties – including a strong latewood temperature signal in tree ring samples from locations where temperature is limiting to growth (Björklund et al., 2019). As the density of the tracheid cell wall should be relatively constant in the conifer xylem (Stamm and Sanders, 1966; Kellogg and Wangaard, 2007), it has been suggested that wood density can be derived from the proportion of cell-wall area to the full cell area (Park and Telewski, 2007) using reflected light images of wood as a substitute to X-radiographs of wood samples (Yanosky and Robinove, 1986; Yanosky et al., 1987). In recent decades, studies using reflected light from tree ring samples have focused on the blue bandwidth of the visible light spectrum due to the strong light-absorbing properties of lignin in this part of the spectrum (McCarroll et al., 2002; Campbell et al., 2007, 2011) as a surrogate for density, and in particular MXBI as the blue reflectance counterpart to MXD (Björklund et al., 2014). MXBI, which represents a measure of absorbed light, can also be referred to as latewood BI (LWBI) or minimum BI (MBI), which typically represent reflected light (Campbell et al., 2007; Björklund et al., 2014; Rydval et al., 2014).

The strong relationship between MXBI, MXD and summer temperatures is related to the thickening and lignification of latewood cell walls. Several studies have shown promising results in terms of temperature associations on par with what would be expected from the traditional MXD parameter (Tene et al., 2011; McCarroll et al., 2013; Wilson et al., 2014; Björklund et al., 2015; Linderholm et al., 2015; Dolgova, 2016; Kaczka et al., 2017; Rydval et al., 2017a,b; 2017a, 2017b; Fuentes et al., 2018; Kaczka et al., 2018; Rydval et al., 2018), however the fidelity of multi-decadal to centennial scale trends in MXBI in relation to MXD has been questioned (Björklund et al., 2014, 2015; Rydval et al., 2014; Buckley et al., 2018). Although the relationship between density and reflected brightness is strongly coupled, it may be distorted for several reasons, such as differential discoloration of cell walls related to heartwood *vs.* sapwood staining (Raven et al., 2005). Treatment of samples using a solvent (e.g. ethanol, acetone) in order to remove resins and other extractives, which may discolour the wood, has been found to be imperfect and so may not eliminate discoloration biases entirely (Sheppard and Wiedenhoeft, 2007; Björklund et al., 2014; Rydval et al., 2014). Björklund et al. (2014) demonstrated that discoloration in latewood BI (LWBI) can be mitigated using earlywood BI (EWBI) by subtracting EWBI from LWBI for each tree-ring, producing a third parameter, the "delta-BI" parameter, later improved upon using a contrast-adjusted delta-BI parameter (Björklund et al., 2015; Linderholm et al., 2015; Fuentes et al., 2018). Despite these possible limitations, especially in the low-frequency domain, MXBI has featured

in large-scale (hemispheric) reconstructions of temperature (Wilson et al., 2016; Anchukaitis et al., 2017).

References

Akaike, H., 1974. A new look at the statistical model identication. Selected Papers of Hirotugu Akaike. Springer, New York, pp. 215–222.

Anchukaitis, K.J., 2017. Tree rings reveal climate change past, present, and future. Proc. Am. Philos. Soc. 161, 244–263.

Anchukaitis, K.J., Wilson, R., Briffa, K.R., Büntgen, U., Cook, E.R., D'Arrigo, R., Davi, N., Esper, J., Frank, D., Gunnarson, B.E., Hegerl, G., Helama, S., Klesse, S., Krusic, P.J., Linderholm, H.W., Myglan, V., Osborn, T.J., Zhang, P., Rydval, M., Schneider, L., Schurer, A., Wiles, G., Zorita, E., 2017. Last millennium Northern Hemisphere summer temperatures from tree rings: Part II, spatially resolved reconstructions. Quat. Sci. Rev. 163, 1–22.

Arbuthnott, J., 1710. An argument for Divine Providence, taken from the constant regularity observed in the births of both sexes. Phil. Trans. 27, 186–190.

Babst, F., Bouriaud, O., Poulter, B., Trouet, V., Girardin, M.P., Frank, D.C., 2019. Twentieth century redistribution in climatic drivers of global tree growth. Sci. Adv. 5, eaat4313.

Babst, F., Poulter, B., Trouet, V., Tan, K., Neuwirth, B., Wilson, R., Carrer, M., Grabner, M., Tegel, W., Levanic, T., Panayotov, M., Urbinati, C., Bouriaud, O., Ciais, P., Frank, D., 2013. Site- and species-specific responses of forest growth to climate across the European continent. Glob. Ecol. Biogeogr. 22, 706–717.

Björklund, J., von Arx, G., Nievergelt, D., Wilson, R., den Bulcke, J.V., Günther, B., Loader, N., Rydval, M., Fonti, P., Scharnweber, T., Andreu-Hayles, L., Büntgen, U., D'Arrigo, R., Davi, N., Mil, T.D., Esper, J., Gärtner, H., Geary, J., Gunnarson, B., Hartl, C., Hevia, A., Song, H., Janecka, K., Kaczka, R., Kirdyanov, A., Kochbeck, M., Yu, L., Meko, M., Mundo, I., Nicolussi, K., Oelkers, R., Pichler, T., Sánchez Salguero, R., Schneider, L., Schweingruber, F., Timonen, M., Trouet, V., Acker, J.V., Verstege, A., Villalba, R., Wilmking, M., Frank, D., 2019. Scientific merits and analytical challenges of tree-ring densitometry. Rev. Geophys. https://doi.org/10.1029/2019RG000642. in press.

Björklund, J., Gunnarson, B.E., Seftigen, K., Esper, J., Linderholm, H., 2014. Blue intensity and density from northern Fennoscandian tree rings, exploring the potential to improve summer temperature reconstructions with earlywood information. Clim. Past 10, 877–885.

Björklund, J., Gunnarson, B.E., Seftigen, K., Zhang, P., Linderholm, H.W., 2015. Using adjusted blue intensity data to attain high-quality summer temperature information: a case study from Central Scandinavia. Holocene 25, 547–556.

Björklund, J., Seftigen, K., Schweingruber, F., Fonti, P., von Arx, G., Bryukhanova, M.V., Cuny, H.E., Carrer, M., Castagneri, D., Frank, D.C., 2017. Cell size and wall dimensions drive distinct variability of earlywood and latewood density in Northern Hemisphere conifers. New Phytol. 216, 728–740.

Böhm, R., Jones, P.D., Hiebl, J., Frank, D., Brunetti, M., Maugeri, M., 2010. The early instrumental warm-bias: a solution for long Central European temperature series 1760–2007. Clim. Change 101, 41–67.

Bonferroni, C.E., 1936. Teoria statistica delle classi e calcolo delle probabilità. Pubblicazioni del R. Istituto Superiore di Scienze Economiche e Commerciali di Firenze 8, 3–62.

Bräker, O., 1981. Alterstrend bei Jahrringdichten und Jahrringbreiten von Nadelholzern und sein Ausgleich. Mitt. Forstl. Bundes-Vers.anst. Wien 142, 75–102.

Breiman, L., Friedman, J., 1985. Estimating optimal transformations for multiple regression and correlation (with discussion). J. Am. Stat. Assoc. 80, 580–619.

Briffa, K., Schweingruber, F., Jones, P., Osborn, T., Shiyatov, S., Vaganov, E., 1998. Reduced sensitivity of recent tree-growth to temperature at high northern latitudes. Nature 391, 678–682.

Briffa, K.R., Osborn, T.J., Schweingruber, F., 2004. Large-scale temperature inferences from tree rings: a review. Glob. Planet. Change 40, 11–26.

Buckley, B.M., Hansen, K.G., Griffin, K.L., Schmiege, S., Oelkers, R., D'Arrigo, R.D., Stahle, D.K., Davi, N., Nguyen, T.Q.T., Le, C.N., Wilson, R.J., 2018. Blue intensity from a tropical conifer's annual rings for climate reconstruction: An ecophysiological perspective. Dendrochronologia 50, 10–22.

Buja, A., Hastie, T.J., Friedman, J., 1989. Linear smoothers and additive models (with discussion). Ann. Stat. 17, 453–555.

Bunde, A., Büntgen, U., Ludescher, J., Luterbacher, J., von Storch, H., 2013. Is there memory in precipitation? Nat. Clim. Change 3, 174–175.

Büntgen, U., Frank, D., Liebhold, A., Johnson, D., Carrer, M., Urbinati, C., Grabner, M., Nicolussi, K., Levanic, T., Esper, J., 2009. Three centuries of insect outbreaks across the European Alps. New Phytol. 182, 929–941.

Büntgen, U., Frank, D., Trouet, V., Esper, J., 2010. Diverse climate sensitivity of Mediterranean tree-ring width and density. Trees 24, 261–273.

Büntgen, U., Frank, D.C., Kaczka, R.J., Verstege, A., Zwijacz-Kozica, T., Esper, J., 2007. Growth responses to climate in a multi-species tree-ring network in the Western Carpathian Tatra Mountains, Poland and Slovakia. Tree Physiol. 27, 689–702.

Büntgen, U., Frank, D.C., Nievergelt, D., Esper, J., 2006. Summer temperature variations in the European Alps, A.D. 755–2004. J. Clim. 19, 5606–5623.

Büntgen, U., Martínez-Peña, F., Aldea, J., Rigling, A., Fischer, E.M., Camarero, J.J., Hayes, M.J., Fatton, V., Egli, S., 2013. Declining pine growth in Central Spain coincides with increasing diurnal temperature range since the 1970s. Glob. Planet. Change 107, 177–185.

Büntgen, U., Raible, C.C., Frank, D., Helama, S., Cunningham, L., Hofer, D., Nievergelt, D., Verstege, A., Timonen, M., Stenseth, N.C., Esper, J., 2011. Causes and consequences of past and projected Scandinavian summer temperatures, 500–2100 AD.

PLoS ONE 6, e25133.

Büntgen, U., Trnka, M., Krusic, P.J., Kyncl, T., Kyncl, J., Luterbacher, J., Zorita, E., Ljungqvist, F.C., Auer, I., Konter, O., Schneider, L., Tegel, W., Štěphánek, P., Brönnimann, S., Hellmann, L., Nievergelt, D., Esper, J., 2015. Tree-ring amplification of the early nineteenth-century summer cooling in Central Europe. J. Clim. 28, 5272–5288.

Büntgen, U., Wacker, G., Lukas, Diego J., Arnold, S., Arseneault, D., Baillie, M., Beer, J., Bernabei, M., Bleicher, N., Boswijk, G., Bräuning, A., Carrer, M., Ljungqvist, F.C., Cherubini, P., Christl, M., Christie, D.A., Clark, P.W., Cook, E.R., D'Arrigo, R., Davi, N., Eggertsson, Ó., Esper, J., Fowler, A.M., Gedalof, Z., Gennaretti, F., Grießinger, J., Grissino-Mayer, H., Grudd, H., Gunnarson, B.E., Hantemirov, R., Herzig, F., Hessl, A., Heussner, K.-U., Jull, A.J.T., Kukarskih, V., Kirdyanov, A., Kolář, T., Krusic, P.J., Kyncl, T., Lara, A., LeQuesne, C., Linderholm, H.W., Loader, N.J., Luckman, B., Miyake, F., Myglan, V.S., Nicolussi, K., Oppenheimer, C., Palmer, J., Panyushkina, I., Pederson, N., Rybníček, M., Schweingruber, F.H., Seim, A., Sigl, M., Churakova (Sidorova), O., Speer, J.H., Synal, H.-A., Tegel, W., Treydte, K., Villalba, R., Wiles, G., Wilson, R., Winship, J., Lawrence, Wunder, J., Yang, B., Young, G.H., 2018. Tree rings reveal globally coherent signature of cosmogenic radiocarbon events in 774 and 993 CE. Nat. Commun. 9, 3605.

Campbell, R., McCarroll, D., Loader, N.J., Grudd, H., Robertson, I., Jalkanen, R., 2007. Blue intensity in *Pinus sylvestris* tree-rings: developing a new palaeoclimate proxy. Holocene 17, 821–828.

Campbell, R., McCarroll, D., Robertson, I., Loader, N.J., Grudd, H., Gunnarson, B., 2011. Blue intensity in *Pinus sylvestris* tree rings: a manual for a new palaeoclimate proxy. Tree Ring Res. 67, 127–134.

Cerrato, R., Salvatore, M.C., Gunnarson, B.E., Linderholm, H.W., Carturan, L., Brunetti, M., De Blasi, F., Baroni, C., 2019. A *Pinus cembra* L. tree-ring record for late spring to late summer temperature in the Rhaetian Alps, Italy. Dendrochronologia 53, 22–31.

Christiansen, B., Ljungqvist, F.C., 2017. Challenges and perspectives for large-scale temperature reconstructions of the past two millennia. Rev. Geophys. 55, 40–96.

Cook, E., Kairiukstis, L., 1990. Method of dendrochronology. Kluwer Academic Publishers, Dordrecht.

Cook, E.R., 1985. A time series analysis approach to tree ring standardization, Ph.D. thesis. University of Arizona, Tucson.

Cook, E.R., Anchukaitis, K.J., Buckley, B.M., D'Arrigo, R.D., Jacoby, G.C., Wright, W.E., 2010. Asian monsoon failure and megadrought during the last millennium. Science 328, 486–489.

Cook, E.R., Briffa, K.R., Meko, D.M., Graybill, D.A., Funkhouser, G., 1995. The 'segment length curse' in long tree-ring chronology development for palaeoclimatic studies. Holocene 5, 229–237.

Cook E.R. and Krusic P.J. 2005. ARSTAN: A tree-ring standardization program based on detrending and autoregressive time series modeling with interactive graphics. Available online at http://www.ldeo.columbia.edu/tree-ring-laboratory/resources/software.

Cook, E.R., Peters, K., 1981. The smoothing spline: a new approach to standardizing forest interior tree-ring width series for dendroclimatic studies. Tree-Ring Bull. 4, 45–53.

Cook, E.R., Peters, K., 1997. Calculating unbiased tree-ring indices for the study of climatic and environmental change. Holocene 7, 361–370.

Cook, E.R., Seager, R., Kushnir, Y., Briffa, K.R., Büntgen, U., Frank, D., Krusic, P.J., Tegel, W., van der Schrier, G., Andreu-Hayles, L., Baillie, M., Baittinger, C., Bleicher, N., Bonde, N., Brown, D., Carrer, M., Cooper, R., Čufar, K., Dittmar, C., Esper, J., Griggs, C., Gunnarson, B., Günther, B., Gutierrez, E., Haneca, K., Helama, S., Herzig, F., Heussner, K.-U., Hofmann, J., Janda, P., Kontic, R., Köse, N., Kyncl, T., Levanič, T., Linderholm, H., Manning, S., Melvin, T.M., Miles, D., Neuwirth, B., Nicolussi, K., Nola, P., Panayotov, M., Popa, I., Rothe, A., Seftigen, K., Seim, A., Svarva, H., Svoboda, M., Thun, T., Timonen, M., Touchan, R., Trotsiuk, V., Trouet, V., Walder, F., Ważny, T., Wilson, R., Zang, C., 2015. Old World megadroughts and pluvials during the Common Era. Sci. Adv. 1, e1500561.

Cook, E.R., Woodhouse, C.A., Eakin, C.M., Meko, D.M., Stahle, D.W., 2004. Long-term aridity changes in the western United States. Science 306, 1015–1018.

D'Arrigo, R., Wilson, R., Liepert, B., Cherubini, P., 2008. On the 'divergence problem' in northern forests: a review of the tree-ring evidence and possible causes. Glob. Planet. Change 60, 289–305.

Dixon, W.J., Mood, A.M., 1946. The statistical sign test. J. Am. Stat. Assoc. 41, 557–566.

Dolgova, E., 2016. June–September temperature reconstruction in the Northern Caucasus based on blue intensity data. Dendrochronologia 39, 17–23.

Dunn, O.J., 1961. Multiple comparisons among means. J. Am. Stat. Assoc. 56, 52–64.

Esper, J., Büntgen, U., Frank, D., Pichler, T., Nicolussi, K., 2007. Updating the Tyrol tree-ring dataset. TRACE 5, 80–84.

Esper, J., Büntgen, U., Frank, D.C., Nievergelt, D., Liebhold, A., 2006. 1200 years of regular outbreaks in alpine insects. Proc. Royal Soc. B 274, 671–679.

Esper, J., Cook, E.R., Krusic, P.J., Peters, K., Schweingruber, F.H., 2003. Tests of the RCS method for preserving low-frequency variability in long tree-ring chronologies. Tree Ring Res. 59, 81–98.

Esper, J., Krusic, P.J., Ljungqvist, F.C., Luterbacher, J., Carrer, M., Cook, E., Davi, N.K., Hartl-Meier, C., Kirdyanov, A., Konter, O., Myglan, V., Timonen, M., Treydte, K., Trouet, V., Villalba, R., Yang, B., Büntgen, U., 2016. Ranking of tree-ring based temperature reconstructions of the past millennium. Quat. Sci. Rev. 145, 134–151.

Esper, J., Schneider, L., Smerdon, J.E., Schöne, B.R., Büntgen, U., 2015. Signals and memory in tree-ring width and density data. Dendrochronologia 35, 62–70.

Esper, J., St George, S., Anchukaitis, K., D'Arrigo, R., Ljungqvist, F.C., Luterbacher, J., Schneider, L., Stoffel, M., Wilson, R., Büntgen, U., 2018. Large-scale, millennial-length temperature reconstructions from tree-rings. Dendrochronologia 50, 81–90.

Fan, J., Gijbels, I., 1996. Local Polynomial Modelling and its Applications. Chapman & Hall, London.

Frank, D., Büntgen, U., Böhm, R., Maugeri, M., Esper, J., 2007. Warmer early

instrumental measurements versus colder reconstructed temperatures: shooting at a moving target. Quat. Sci. Rev. 26, 3298–3310.

Frank, D., Esper, J., 2005. Characterization and climate response patterns of a high-elevation, multi-species tree-ring network in the European Alps. Dendrochronologia 22, 107–121.

Frank, D., Poulter, B., Saurer, M., Esper, J., Huntingford, C., Helle, G., Treydte, K., Zimmermann, N., Schleser, G., Ahlström, A., Ciais, P., Friedlingstein, P., Levis, S., Lomas, M., Sitch, S., Viovy, N., Andreu-Hayles, L., Bednarz, Z., Berninger, F., Boettger, T., D'Alessandro, C., Daux, V., Filot, M., Grabner, M., Gutierrez, E., Haupt, M., Hilasvuori, E., Jungner, H., Kalela-Brundin, M., Krapiec, M., Leuenberger, M., Loader, N., Marah, H., Masson-Delmotte, V., Pazdur, A., Pawelczyk, S., Pierre, M., Planells, O., Pukiene, R., Reynolds-Henne, E., Rinne, K., Saracino, A., Sonninen, E., Stievenard, M., Switsur, V., Szczepanek, M., Szychowska-Krapiec, E., Todaro, L., Waterhouse, J., Weigl, M., 2015. Water-use efficiency and transpiration across European forests during the Anthropocene. Nat. Clim. Change 5, 579–583.

Franke, J., Frank, D., Raible, C.C., Esper, J., Brönnimann, S., 2013. Spectral biases in tree-ring climate proxies. Nature Clim. Change 3, 360–364.

Fritts, H., 1976. Tree Rings and Climate. Academic Press, New York.

Fuentes, M., Salo, R., Björklund, J., Seftigen, K., Zhang, P., Gunnarson, B., Aravena, J.-C., Linderholm, H.W., 2018. A 970-year-long summer temperature reconstruction from Rogen, west-central Sweden, based on blue intensity from tree rings. Holocene 28, 254–266.

Galván, J.D., Camarero, J.J., Ginzler, C., Büntgen, U., 2014. Spatial diversity of recent trends in Mediterranean tree growth. Environ. Res. Lett. 9, 084001.

Graybill, D.A., Idso, S.B., 1993. Detecting the aerial fertilization effect of atmospheric CO_2 enrichment in tree-ring chronologies. Global. Biogeochem. Cy. 7, 81–95.

Grissino-Mayer, H.D., 1993. An updated list of species used in tree-ring research. Tree-Ring Bull. 53, 17–43.

Gunnarson, B.E., Josefsson, T., Linderholm, H.W., Östlund, L., 2012. Legacies of pre-industrial land use can bias modern tree-ring climate calibrations. Clim. Res. 53, 63–76.

Hastie, T.J., Tibshirani, R., 1990. Generalized Additive Models. Chapman & Hall, London.

He, H., Jansson, P.-E., Svensson, M., Björklund, J., Tarvainen, L., Klemedtsson, L., Kasimir, Å., 2016. Forests on drained agricultural peatland are potentially large sources of greenhouse gases – insights from a full rotation period simulation. Biogeosciences 13, 2305–2318.

Hellmann, L., Agafonov, L., Ljungqvist, F.C., Churakova, O., Düthorn, E., Esper, J., Hülsmann, L., Kirdyanov, A.V., Moiseev, P., Myglan, V.S., Nikolaev, A.N., Reinig, F., Schweingruber, F.H., Solomina, O., Tegel, W., Büntgen, U., 2016. Diverse growth trends and climate responses across Eurasia's boreal forest. Environ. Res. Lett. 11, 074021.

Hoaglin, D.C., Mosteller, F., Tukey, J.W., 1983. Understanding Robust and Exploratory Data Analysis. Wiley, New York.

Jacoby, G.C., D'Arrigo, R.D., 1995. Tree ring width and density evidence of climatic and potential forest change in Alaska. Global Biogeochem. Cy. 9, 227–234.

Jones, P., Lister, D., Osborn, T., Harpham, C., Salmon, M., Morice, C., 2012. Hemispheric and large-scale land-surface air temperature variations: An extensive revision and an update to 2010. J. Geophys. Res. 117, D05127.

Jones, P., Osborn, T., Briffa, K., 1997. Estimating sampling errors in large-scale temperature averages. J. Clim. 10, 2548–2568.

Kaczka, R., Spyt, B., Janecka, K., Musioł, R., 2017. The Blue Intensity proxy for 400 years growing season temperature reconstruction from the Tatra Mountains. TRACE 15, 23–30.

Kaczka, R.J., Spyt, B., Janecka, K., Beil, I., Büntgen, U., Scharnweber, T., Nievergelt, D., Wilmking, M., 2018. Different maximum latewood density and blue intensity measurements techniques reveal similar results. Dendrochronologia 49, 94–101.

Keenan, T.F., Hollinger, D.Y., Bohrer, G., Dragoni, D., Munger, J.W., Schmid, H.P., Richardson, A.D., 2013. Increase in forest water-use efficiency as atmospheric carbon dioxide concentrations rise. Nature 499, 324–327.

Kellogg, R.M., Wangaard, F.F., 2007. Variation in the cell-wall density of wood. Wood Fiber Sci. 1, 180–204.

Kennedy, J., Rayner, N., Smith, R., Parker, D., Saunby, M., 2011a. Reassessing biases and other uncertainties in sea surface temperature observations measured *in situ* since 1850: 1. Measurement and sampling uncertainties. J. Geophys. Res. 116, D14103.

Kennedy, J., Rayner, N., Smith, R., Parker, D., Saunby, M., 2011b. Reassessing biases and other uncertainties in sea surface temperature observations measured *in situ* since 1850: 2. Biases and homogenization. J. Geophys. Res. 116, D14104.

Kirdyanov, A.V., Vaganov, E.A., Hughes, M.K., 2007. Separating the climatic signal from tree-ring width and maximum latewood density records. Trees 21, 37–44.

Klesse, S., Babst, F., Lienert, S., Spahni, R., Joos, F., Bouriaud, O., Carrer, M., Di Filippo, A., Poulter, B., Trotsiuk, V., Wilson, R., Frank, D.C., 2018. A combined tree ring and vegetation model assessment of European forest growth sensitivity to interannual climate variability. Global Biogeochem. Cycles 32, 1226–1240.

Klippel, L., St George, S., Büntgen, U., Krusic, P.J., Esper, J., 2019. Differing pre-industrial cooling trends between tree-rings and lower-resolution temperature proxies. Clim. Past Discuss. 2019, 1–21.

Konter, O., Büntgen, U., Carrer, M., Timonen, M., Esper, J., 2016. Climate signal age effects in boreal tree-rings: Lessons to be learned for paleoclimatic reconstructions. Quat. Sci. Rev. 142, 164–172.

Körner, C., Morgan, J., Norby, R., 2007. CO_2 fertilization: When, where, how much? In Terrestrial ecosystems in a changing world. Springer, Berlin, pp. 9–21.

Linderholm, H.W., Björklund, J., Seftigen, K., Gunnarson, B.E., Fuentes, M., 2015. Fennoscandia revisited: a spatially improved tree-ring reconstruction of summer temperatures for the last 900 years. Clim. Dyn. 45, 933–947.

Linderholm, H.W., Gunnarson, B.E., 2019. Were medieval warm-season temperatures in Jämtland, central Scandinavian Mountains, lower than previously estimated? Dendrochronologia 57, 125607.

Ljungqvist, F.C., Krusic, P.J., Sundqvist, H.S., Zorita, E., Brattström, G., Frank, D., 2016. Northern Hemisphere hydroclimate variability over the past twelve centuries. Nature 532, 94–98.

Ljungqvist, F.C., Seim, A., Krusic, P.J., González-Rouco, J.F., Werner, J.P., Cook, E.R., Zorita, E., Luterbacher, J., Xoplaki, E., Destouni, G., García-Bustamante, E., Aguilar, C.A.M., Seftigen, K., Wang, J., Gagen, M.H., Esper, J., Solomina, O., Fleitmann, D., Büntgen, U., 2019a. European warm-season temperature and hydroclimate since 850 CE. Environ. Res. Lett. 14, 084015.

Ljungqvist, F.C., Zhang, Q., Brattström, G., Krusic, P.J., Seim, A., Li, Q., Zhang, Q., Moberg, A., 2019b. Centennial-scale temperature change in last millennium simulations and proxy-based reconstructions. J. Clim. 32, 2441–2482.

Matalas, N.C., 1962. Statistical properties of tree ring data. Hydrolog. Sci. J. 7, 39–47.

McCarroll, D., Loader, N.J., Jalkanen, R., Gagen, M.H., Grudd, H., Gunnarson, B.E., Kirchhefer, A.J., Friedrich, M., Linderholm, H.W., Lindholm, M., Boettger, T., Los, S.O., Remmele, S., Kononov, Y.M., Yamazaki, Y.H., Young, G.H., Zorita, E., 2013. A 1200-year multiproxy record of tree growth and summer temperature at the northern pine forest limit of Europe. Holocene 23, 471–484.

McCarroll, D., Pettigrew, E., Luckman, A., Guibal, F., Edouard, J.-L., 2002. Blue reflectance provides a surrogate for latewood density of high-latitude pine tree rings. Arct. Antarct. Alp. Res. 34, 450–453.

Melvin, T.M., Briffa, K.R., 2008. A "signal-free" approach to dendroclimatic standardisation. Dendrochronologia 26, 71–86.

Melvin, T.M., Grudd, H., Briffa, K.R., 2013. Potential bias in 'updating' tree-ring chronologies using regional curve standardisation: Re-processing 1500 years of Torneträsk density and ring-width data. Holocene 23, 364–373.

Moberg, A., Alexandersson, H., Bergström, H., Jones, P.D., 2003. Were southern Swedish summer temperatures before 1860 as warm as measured? Int. J. Climatol. 23, 1495–1521.

Morice, C.P., Kennedy, J.J., Rayner, N.A., Jones, P.D., 2012. Quantifying uncertainties in global and regional temperature change using an ensemble of observational estimates: The HadCRUT4 data set. J. Geophys. Res. 117, D08101.

Park, W.-K., Telewski, F.W., 2007. Measuring maximum latewood density by image analysis at the cellular level. Wood Fiber Sci. 25, 326–332.

R Core Team, 2018. R: A Language and Environment for Statistical Computing. R Foundation for Statistical Computing, Vienna, Austria.

Raven, P.H., Evert, R.F., Eichhorn, S.E., 2005. Biology of Plants. Macmillan, London.

Rydval, M., Druckenbrod, D., Anchukaitis, K.J., Wilson, R., 2016. Detection and removal of disturbance trends in tree-ring series for dendroclimatology. Can. J. Forest Res. 46, 387–401.

Rydval, M., Druckenbrod, D.L., Svoboda, M., Trotsiuk, V., Janda, P., Mikoláš, M., Čada, V., Bače, R., Teodosiu, M., Wilson, R., 2018. Influence of sampling and disturbance history on climatic sensitivity of temperature-limited conifers. Holocene 28, 1574–1587.

Rydval, M., Gunnarson, B.E., Loader, N.J., Cook, E.R., Druckenbrod, D.L., Wilson, R., 2017a. Spatial reconstruction of Scottish summer temperatures from tree rings. Int. J. Climatol. 37, 1540–1556.

Rydval, M., Larsson, L.-Å., McGlynn, L., Gunnarson, B.E., Loader, N.J., Young, G.H., Wilson, R., 2014. Blue intensity for dendroclimatology: should we have the blues? Experiments from Scotland. Dendrochronologia 32, 191–204.

Rydval, M., Loader, N.J., Gunnarson, B.E., Druckenbrod, D.L., Linderholm, H.W., Moreton, S.G., Wood, C.V., Wilson, R., 2017b. Reconstructing 800 years of summer temperatures in Scotland from tree rings. Clim. Dyn. 49, 2951–2974.

Scharnweber, T., Heußner, K.-U., Smiljanic, M., Heinrich, I., van der Maaten-Theunissen, M., van der Maaten, E., Struwe, T., Buras, A., Wilmking, M., 2019. Removing the no-analogue bias in modern accelerated tree growth leads to stronger medieval drought. Sci. Rep. 9, 2509.

Schneider, L., Smerdon, J.E., Büntgen, U., Wilson, R.J., Myglan, V.S., Kirdyanov, A.V., Esper, J., 2015. Revising midlatitude summer temperatures back to AD 600 based on a wood density network. Geophys. Res. Lett. 42, 4556–4562.

Schulman, E., 1956. Dendroclimatic Changes in Semiarid America. University of Arizona Press, Tucson.

Schultz, J., Beck, C., Menz, G., Neuwirth, B., Ohlwein, C., Philipp, A., 2015. Sensitivity of proxies on non-linear interactions in the climate system. Sci. Rep. 5, 18560.

Schweingruber, F., 1988. Tree Rings: Basics and Applications of Dendrochronology. Kluwer Academic Publishers, Dodrecht.

Schweingruber, F., Fritts, H., Bräker, O., Drew, L., Schär, E., 1978. The X-ray technique as applied to dendroclimatology. Tree-Ring Bull. 38, 61–91.

Schweingruber, F.H., Bartholin, T., Schaur, E., Briffa, K.R., 1988. Radiodensitometric-dendroclimatological conifer chronologies from Lapland (Scandinavia) and the Alps (Switzerland). Boreas 17, 559–566.

Seim, A., Omurova, G., Azisov, E., Musuraliev, K., Aliev, K., Tulyaganov, T., Nikolyai, L., Botman, E., Helle, G., Liñan, I.D., Jivcov, S., Linderholm, H.W., 2016. Climate change increases drought stress of juniper trees in the mountains of central Asia. PLoS ONE 11, e0153888.

Sheppard, P.R., Wiedenhoeft, A., 2007. An advancement in removing extraneous color from wood for low-magnification reflected-light image analysis of conifer tree rings. Wood Fiber Sci. 39, 173–183.

Speer, J.H., 2010. Fundamentals of tree-ring research. University of Arizona Press, Tucson.

St George, S., 2014. An overview of tree-ring width records across the Northern Hemisphere. Quat. Sci. Rev. 95, 132–150.

St George, S., Ault, T.R., 2014. The imprint of climate within Northern Hemisphere trees. Quat. Sci. Rev. 89, 1–4.

Stamm, A.J., Sanders, H., 1966. Specific gravity of wood substance of loblolly pine as affected by chemical composition. Tappi 49, 397–400.

Støve, B., Ljungqvist, F.C., Thejll, P., 2012. A test for nonlinearity in temperature proxy

records. J. Clim. 25, 7173–7186.

Tene, A., Tobin, B., Dyckmans, J., Ray, D., Black, K., Nieuwenhuis, M., 2011. Assessment of tree response to drought: validation of a methodology to identify and test proxies for monitoring past environmental changes in trees. Tree Physiol. 31, 309–322.

Vaganov, E.A., Hughes, M.K., Shashkin, A.V., 2006. Growth dynamics of conifer tree rings: images of past and future environments. Springer Science & Business Media, Berlin.

Weiner, J., Thomas, S.C., 2001. The nature of tree growth and the "age-related decline in forest productivity". Oikos 94, 374–376.

Wigley, T.M., Briffa, K.R., Jones, P.D., 1984. On the average value of correlated time series, with applications in dendroclimatology and hydrometeorology. J. Appl. Meteorol. Climatol. 23, 201–213.

Wilson, R., Anchukaitis, K., Briffa, K.R., Büntgen, U., Cook, E., D'Arrigo, R., Davi, N., Esper, J., Frank, D., Gunnarson, B., Hegerl, G., Helama, S., Klesse, S., Krusic, P.J., W, L.H., Myglan, V., Osborn, T.J., Rydval, M., Zorita, E., 2016. Last millennium northern hemisphere summer temperatures from tree rings: Part I: The long term context. Quat. Sci. Rev. 134, 1–18.

Wilson, R., D'Arrigo, R., Andreu-Hayles, L., Oelkers, R., Wiles, G., Anchukaitis, K., Davi, N., 2017a. Experiments based on blue intensity for reconstructing North Pacific temperatures along the Gulf of Alaska. Clim. Past 13, 1007–1022.

Wilson, R., D'Arrigo, R., Buckley, B., Büntgen, U., Esper, J., Frank, D., Luckman, B., Payette, S., Vose, R., Youngblut, D., 2007. A matter of divergence: tracking recent warming at hemispheric scales using tree ring data. J. Geophys. Res. 112, D17103.

Wilson, R., Rao, R., Rydval, M., Wood, C., Larsson, L.-Å., Luckman, B.H., 2014. Blue Intensity for dendroclimatology: The BC blues: A case study from British Columbia. Canada. Holocene 24, 1428–1438.

Wilson, R., Wilson, D., Rydval, M., Crone, A., Büntgen, U., Clark, S., Ehmer, J., Forbes, E., Fuentes, M., Gunnarson, B.E., Linderholm, H.W., Nicolussi, K., Wood, C., Mills, C., 2017b. Facilitating tree-ring dating of historic conifer timbers using Blue Intensity. J. Archaeol. Sci. 78, 99–111.

Wood, S., 2017. Generalized Additive Models: An Introduction with R. 2nd ed. Chapman and Hall/CRC, London.

Yanosky, T., Robinove, C., Clark, R., 1987. Progress in the image analysis of tree rings. In: In International Symposium on Ecological Aspects of Tree-Ring Analysis. US Department of Energy, Office of Energy Research. pp. 658–665.

Yanosky, T.M., Robinove, C.J., 1986. Digital image measurement of the area and anatomical structure of tree rings. Can. J. Bot. 64, 2896–2902.

Zhang, H., Yuan, N., Esper, J., Werner, J.P., Xoplaki, E., Büntgen, U., Treydte, K., Luterbacher, J., 2015. Modified climate with long term memory in tree ring proxies. Environ. Res. Lett. 10, 084020.

Zhu, Z., Piao, S., Myneni, R.B., Huang, M., Zeng, Z., Canadell, J.G., Ciais, P., Sitch, S., Friedlingstein, P., Arneth, A., Cao, C., Cheng, L., Kato, E., Koven, C., Li, Y., Lian, X., Liu, Y., Liu, R., Mao, J., Pan, Y., Peng, S., Penuelas, J., Poulter, B., Pugh, T.A.M., Stocker, B.D., Viovy, N., Wang, X., Wang, Z., Yingping Xiao, Yang, H., Zaehle, S., Zeng, N., 2016. Greening of the Earth and its drivers. Nat. Clim. Change 6, 791–795.